Ferguson, M. C., S. F. Tóth, J. T. Clarke, A. L. Willoughby, A. A. Brower, and T. P. White

Biologically Important Areas for Bowhead Whales (*Balaena mysticetus*):
Optimal Site Selection with Integer Programming

Appendix S1

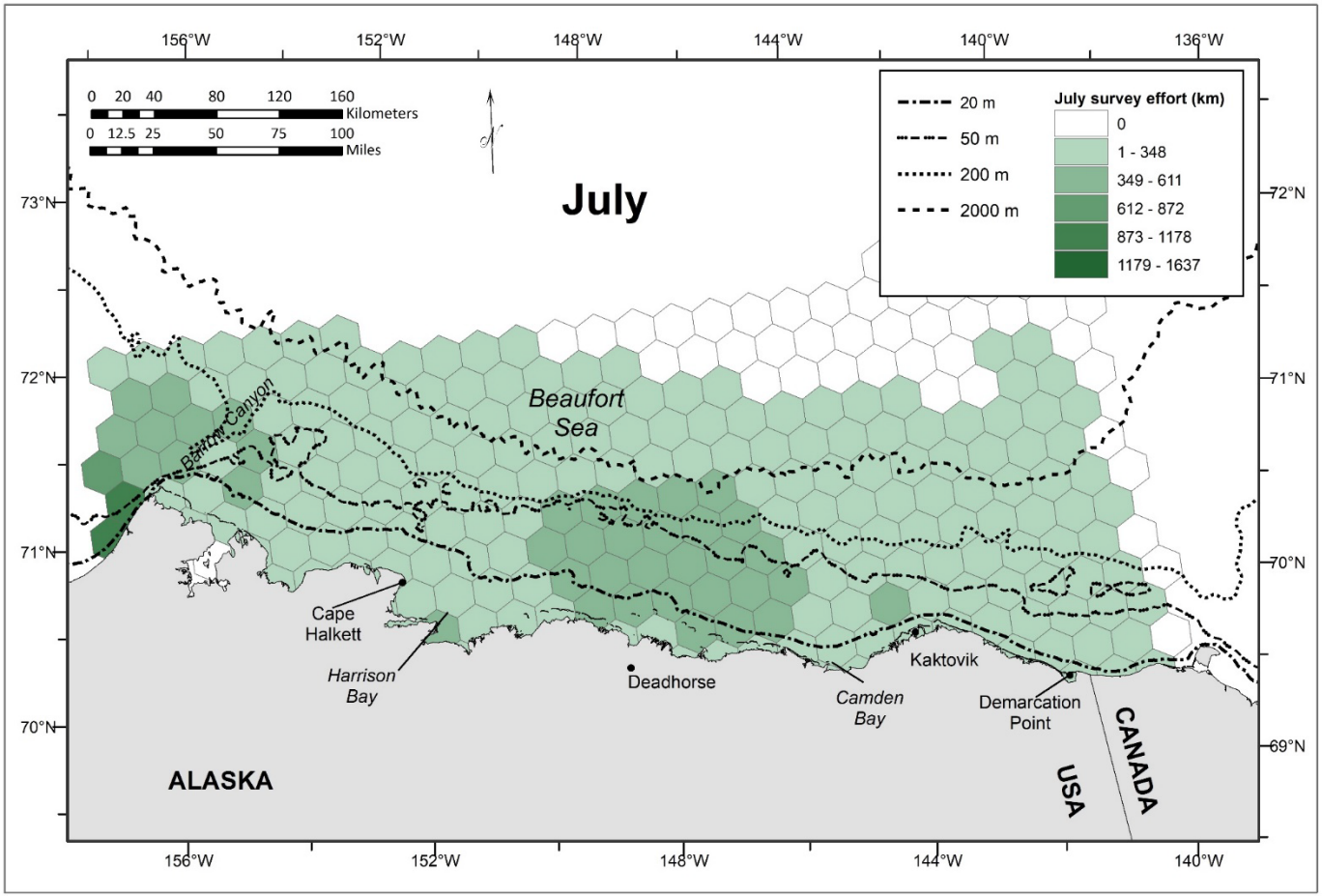

Figure S1A. July aerial survey effort (transect and Cetacean Aggregation Protocols passing modes) in the western Beaufort Sea, pooled across years 2000-2019.

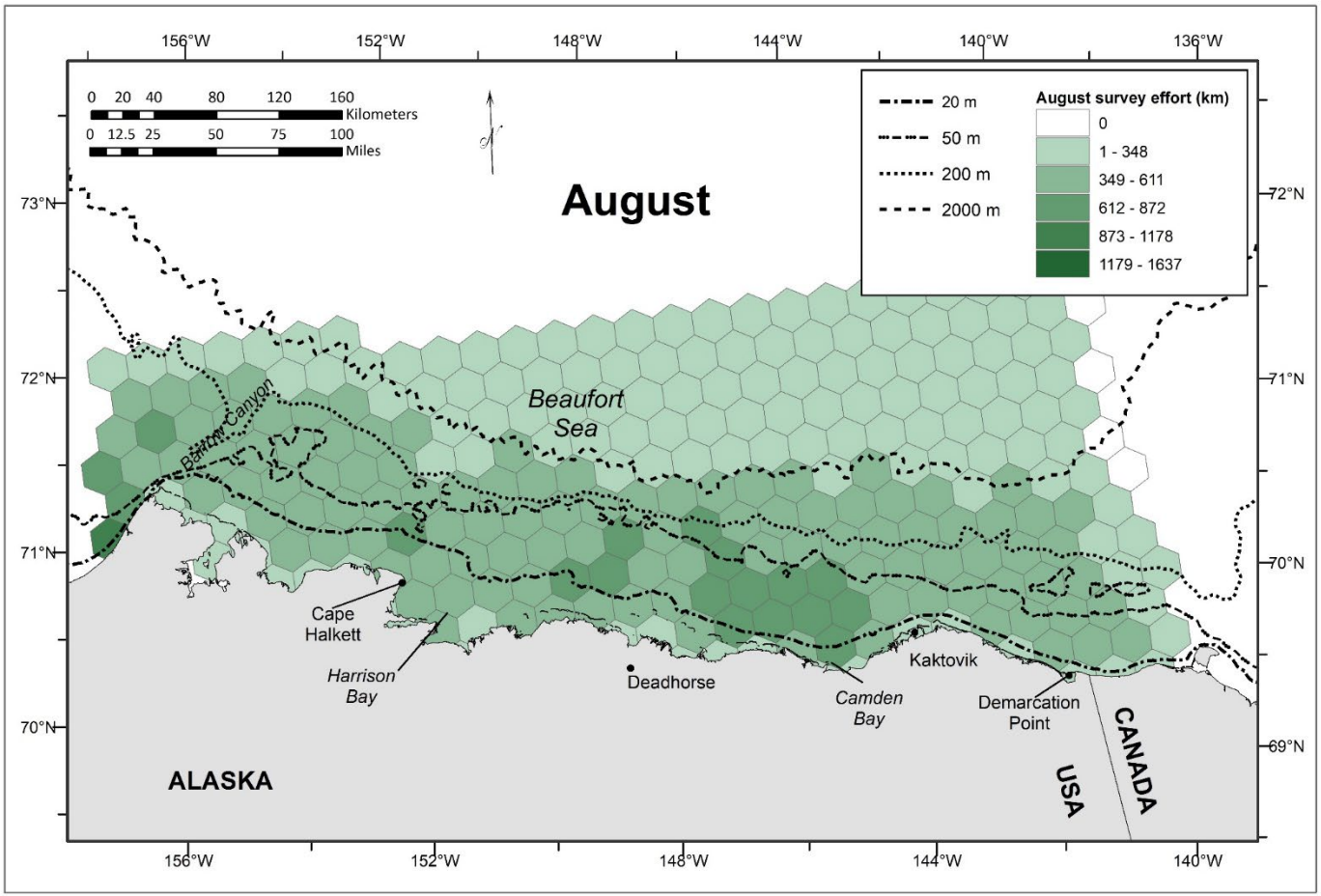

Figure S1B. August aerial survey effort (transect and Cetacean Aggregation Protocols passing modes) in the western Beaufort Sea, pooled across years 2000-2019.

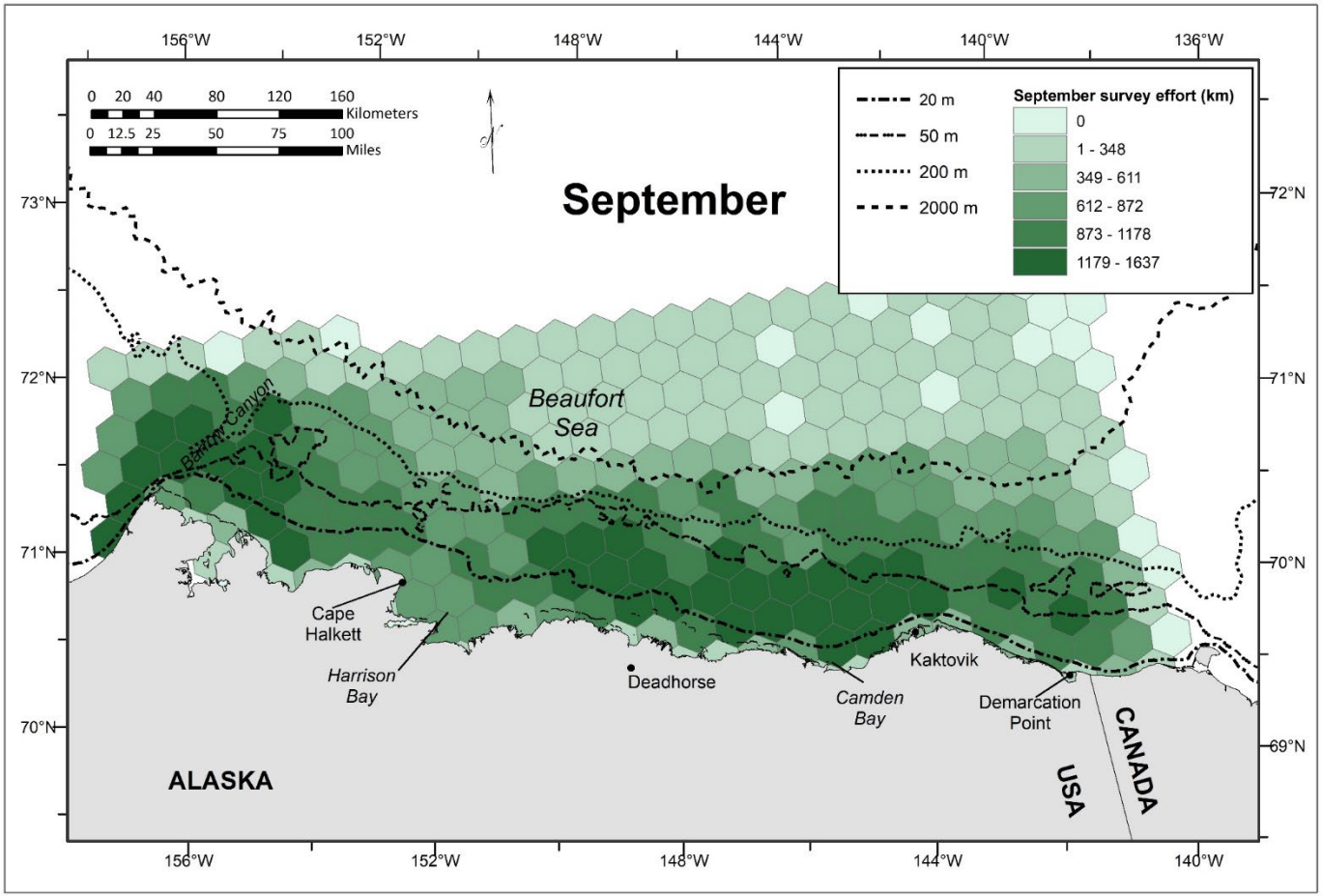

Figure S1C. September aerial survey effort (transect and Cetacean Aggregation Protocols passing modes) in the western Beaufort Sea, pooled across years 2000-2019.

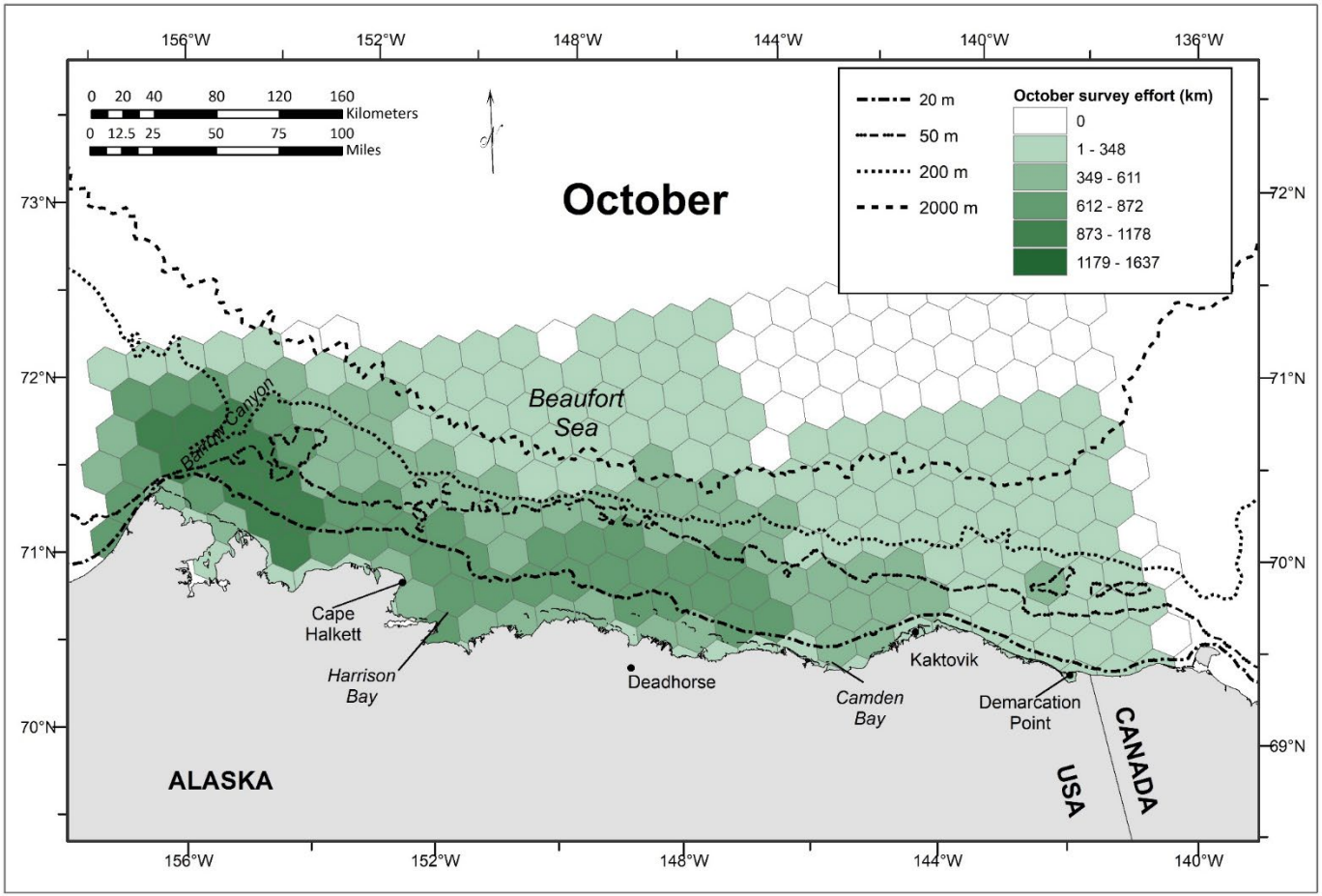

Figure S1D. October aerial survey effort (transect and Cetacean Aggregation Protocols passing modes) in the western Beaufort Sea, pooled across years 2000-2019.

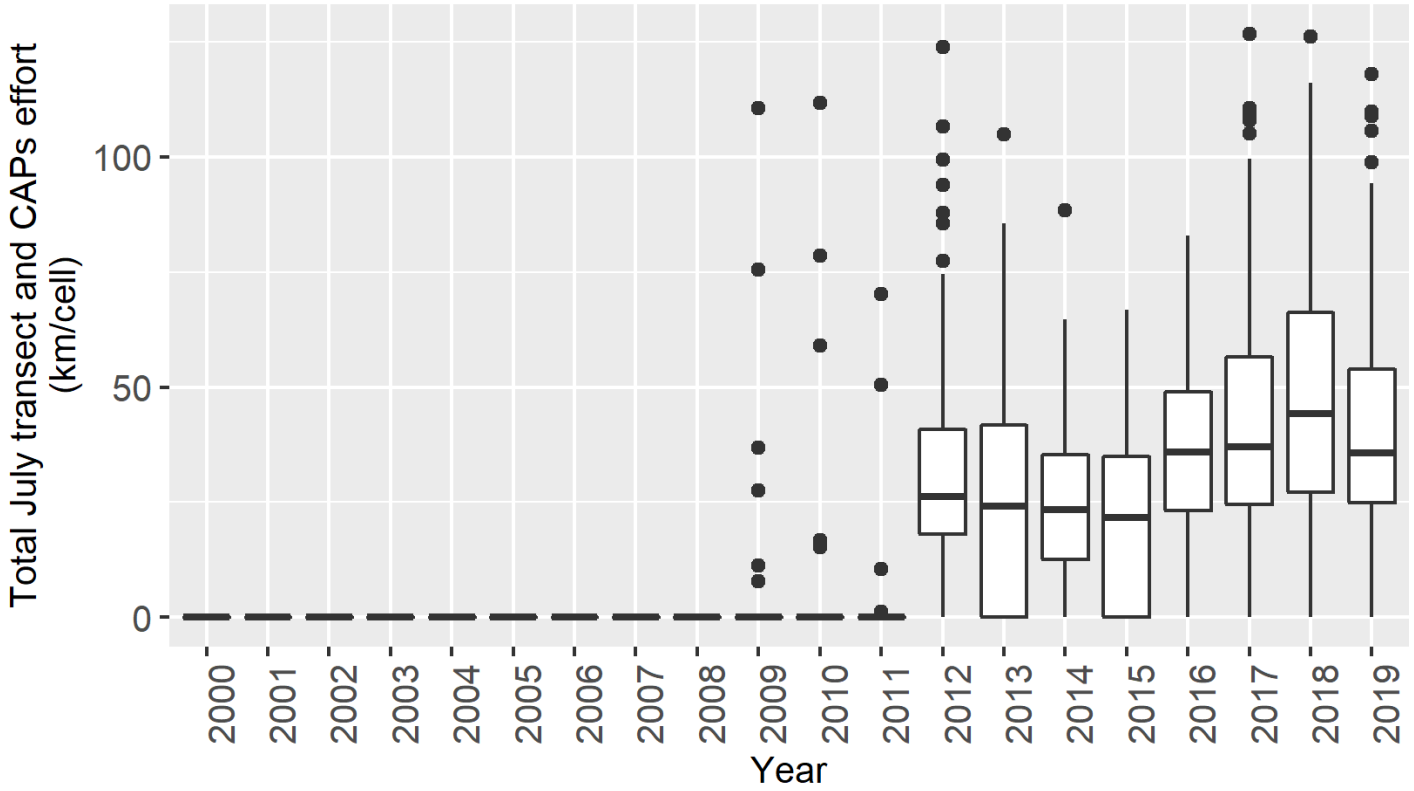

Figure S2A. Distribution of July survey effort (transect and Cetacean Aggregation Protocols passing modes) by year (2000 to 2019) in the western Beaufort Sea. For each year, five summary statistics are presented: the median, 25th percentile (lower hinge), 75th percentile (upper hinge), lower whisker, and upper whisker. The lower whisker extends from the hinge to the smallest value at most 1.5 * IQR of the hinge, where IQR is the inter-quartile range, or distance between the 25th and 75th percentiles. The upper whisker extends from the hinge to the largest value no further than 1.5 * IQR from the hinge. Outliers (data beyond the end of the whiskers) are plotted individually.

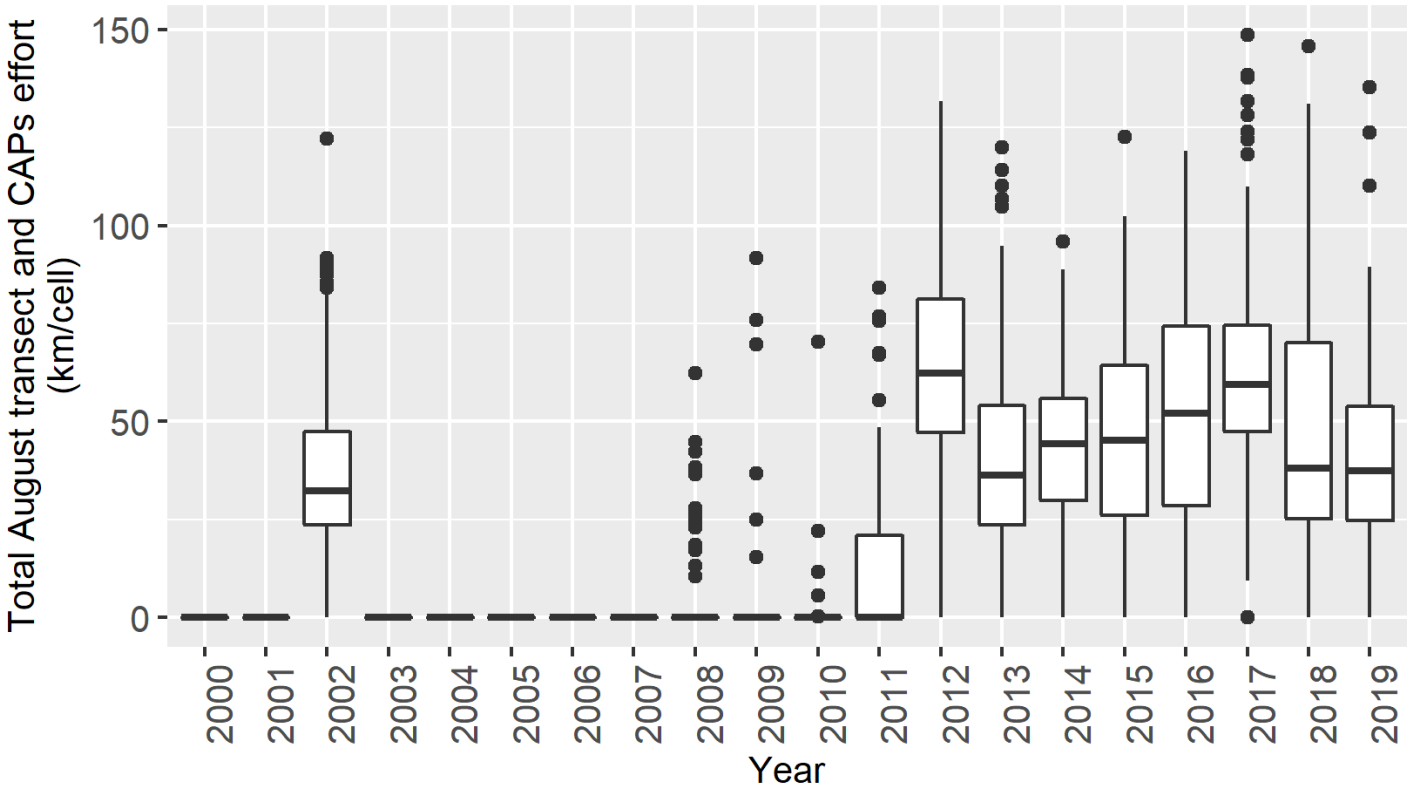

Figure S2B. Distribution of August survey effort (transect and Cetacean Aggregation Protocols passing modes) by year (2000 to 2019) in the western Beaufort Sea. For each year, five summary statistics are presented: the median, 25th percentile (lower hinge), 75th percentile (upper hinge), lower whisker, and upper whisker. The lower whisker extends from the hinge to the smallest value at most 1.5 * IQR of the hinge, where IQR is the inter-quartile range, or distance between the 25th and 75th percentiles. The upper whisker extends from the hinge to the largest value no further than 1.5 * IQR from the hinge. Outliers (data beyond the end of the whiskers) are plotted individually.

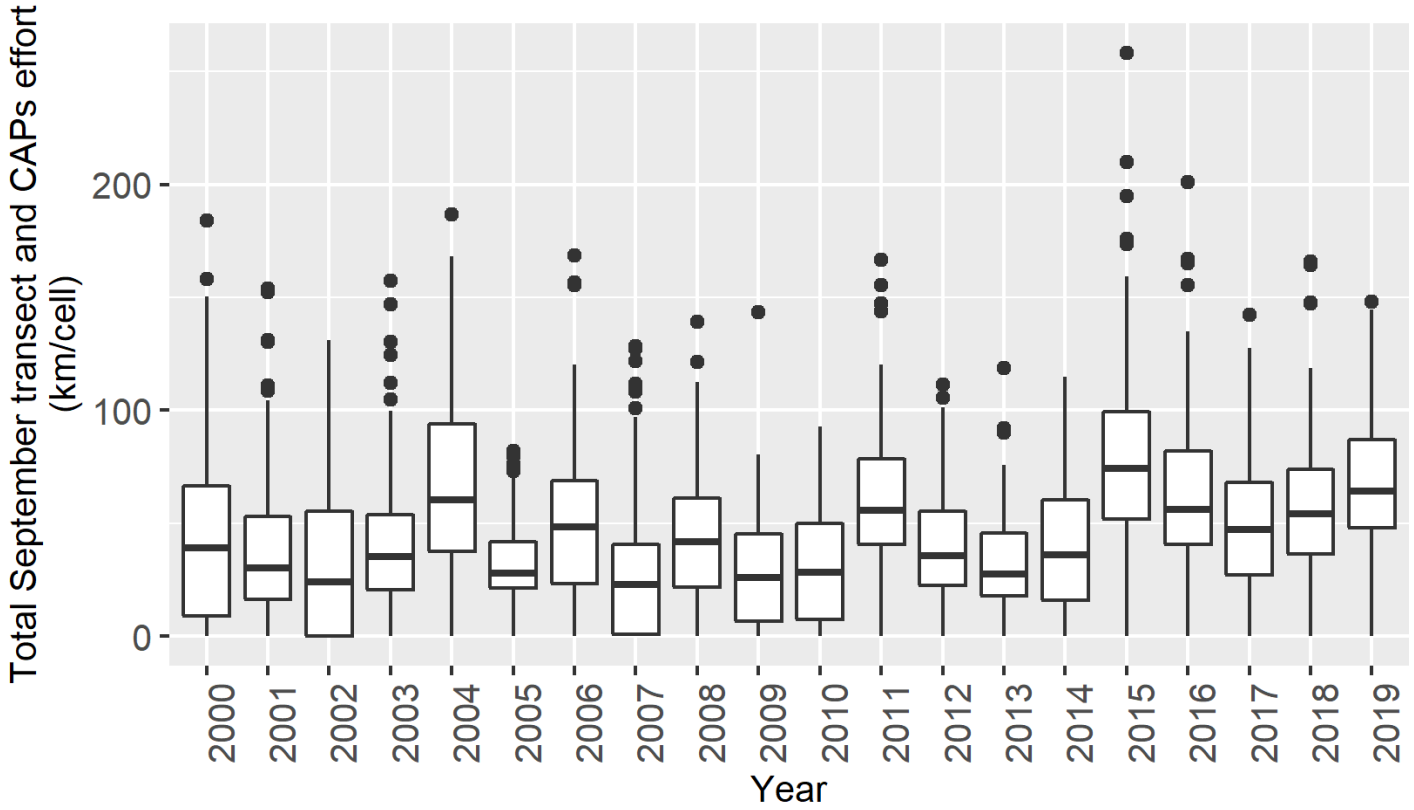

Figure S2C. Distribution of September survey effort (transect and Cetacean Aggregation Protocols passing modes) by year (2000 to 2019) in the western Beaufort Sea. For each year, five summary statistics are presented: the median, 25th percentile (lower hinge), 75th percentile (upper hinge), lower whisker, and upper whisker. The lower whisker extends from the hinge to the smallest value at most 1.5 * IQR of the hinge, where IQR is the inter-quartile range, or distance between the 25th and 75th percentiles. The upper whisker extends from the hinge to the largest value no further than 1.5 * IQR from the hinge. Outliers (data beyond the end of the whiskers) are plotted individually.

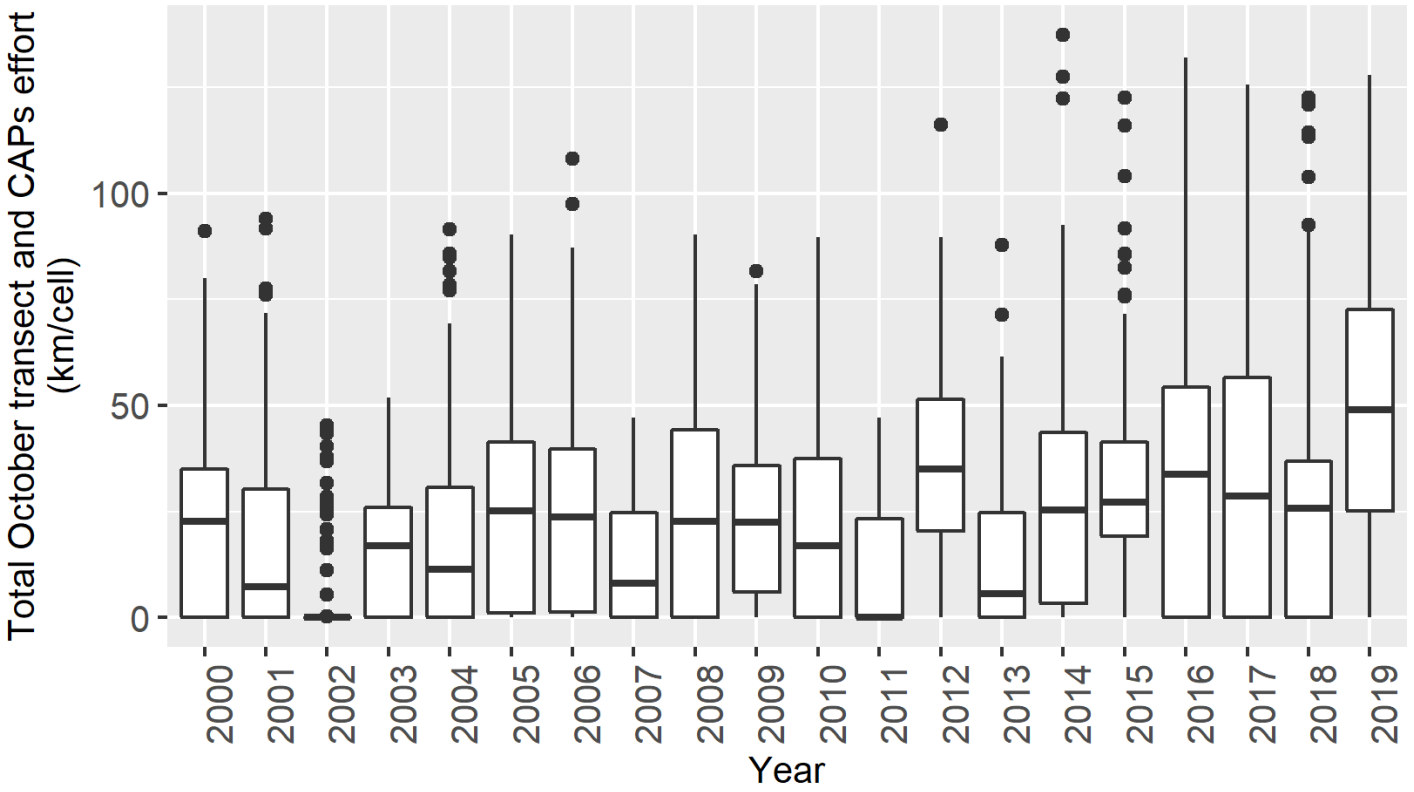

Figure S2D. Distribution of October survey effort (transect and Cetacean Aggregation Protocols passing modes) by year (2000 to 2019) in the western Beaufort Sea. For each year, five summary statistics are presented: the median, 25th percentile (lower hinge), 75th percentile (upper hinge), lower whisker, and upper whisker. The lower whisker extends from the hinge to the smallest value at most 1.5 * IQR of the hinge, where IQR is the inter-quartile range, or distance between the 25th and 75th percentiles. The upper whisker extends from the hinge to the largest value no further than 1.5 * IQR from the hinge. Outliers (data beyond the end of the whiskers) are plotted individually.

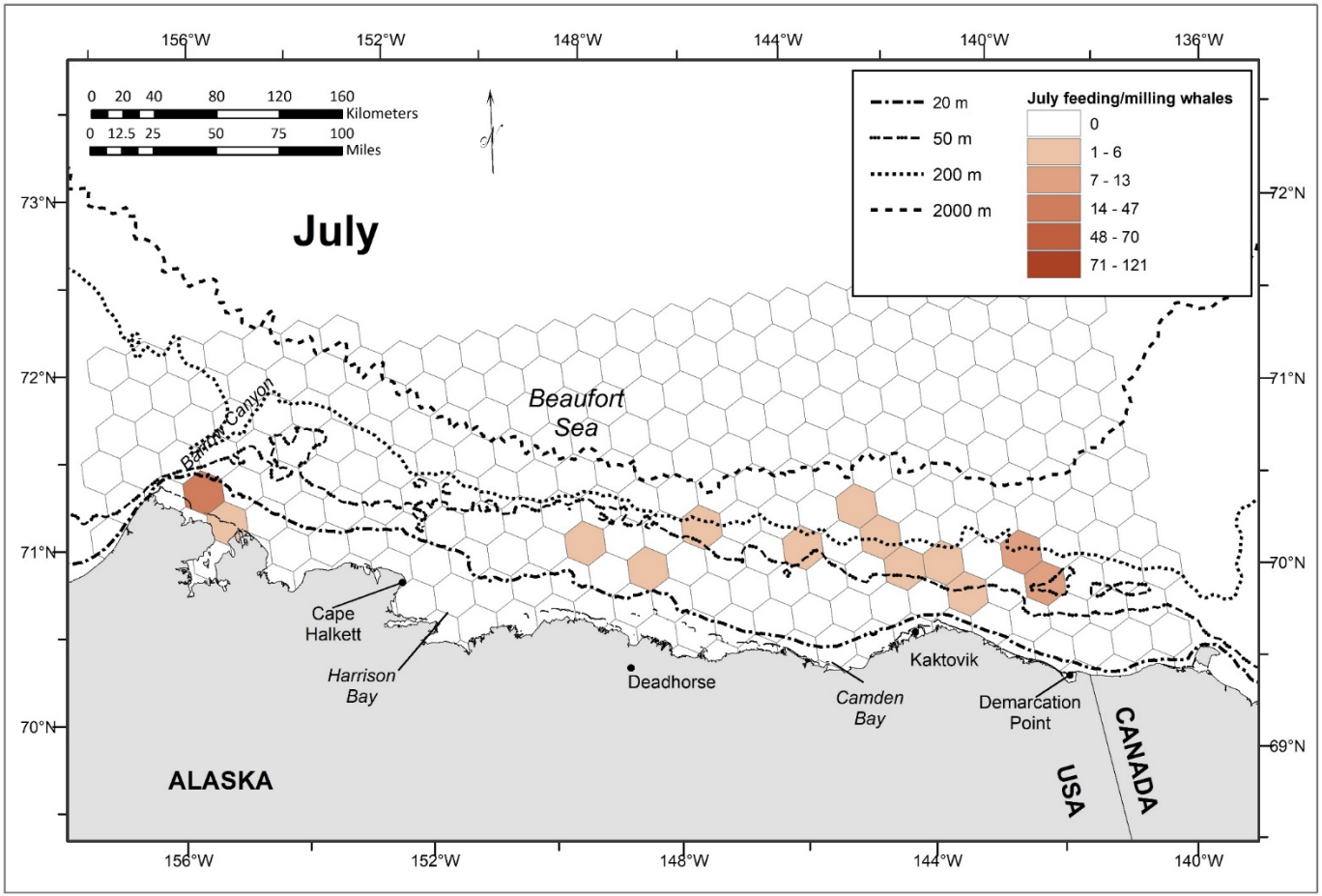

Figure S3A. Number of sightings of feeding and milling bowhead whales during transect and Cetacean Aggregation Protocols passing modes in the western Beaufort Sea during July from 2000 to 2019.

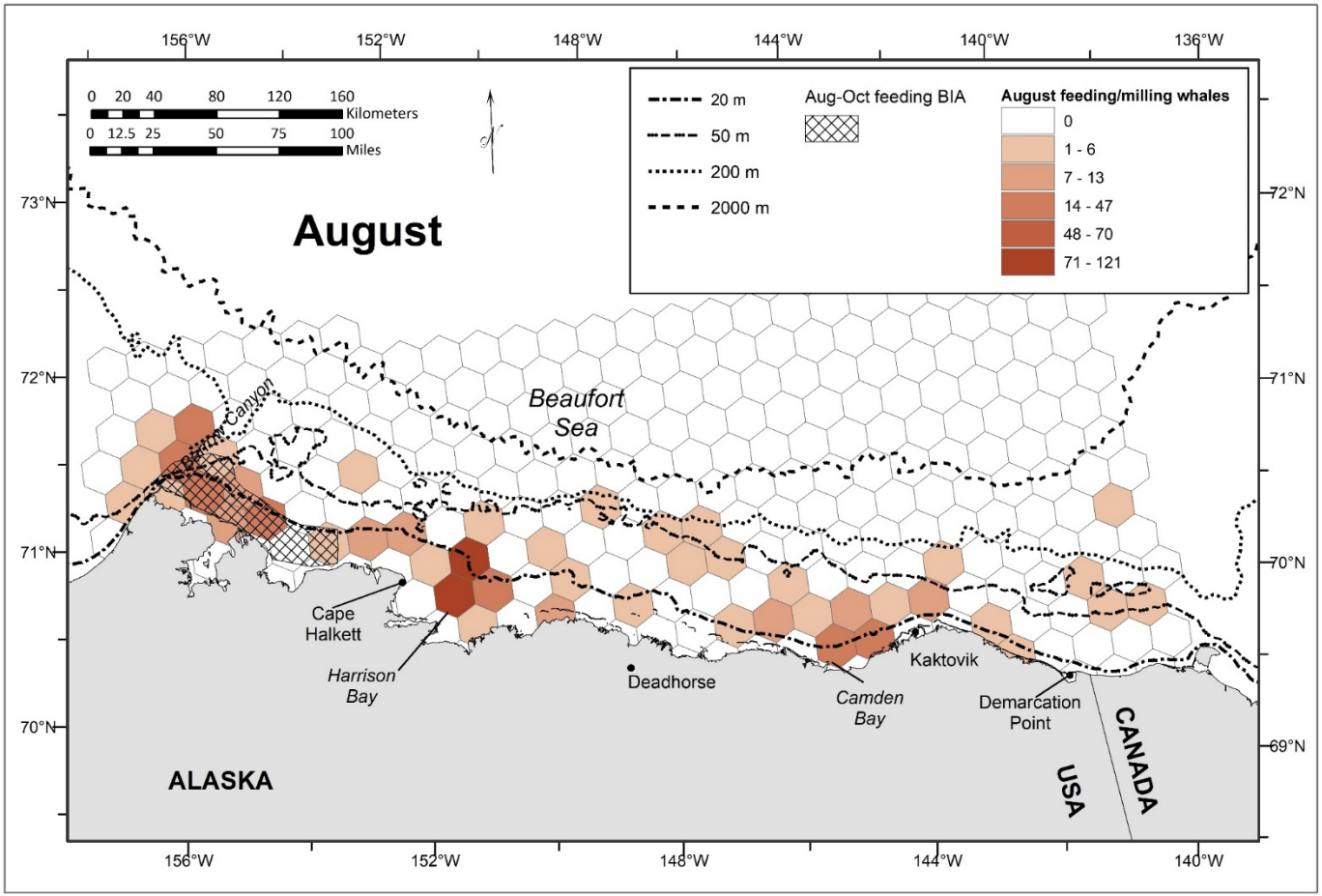

Figure S3B. Number of sightings of feeding and milling bowhead whales during transect and Cetacean Aggregation Protocols passing modes in the western Beaufort Sea during August from 2000 to 2019. Polygons representing the Biologically Important Areas (BIAs) for feeding bowhead whales that were delineated during the initial BIA effort (Clarke et al. 2015) are also shown.

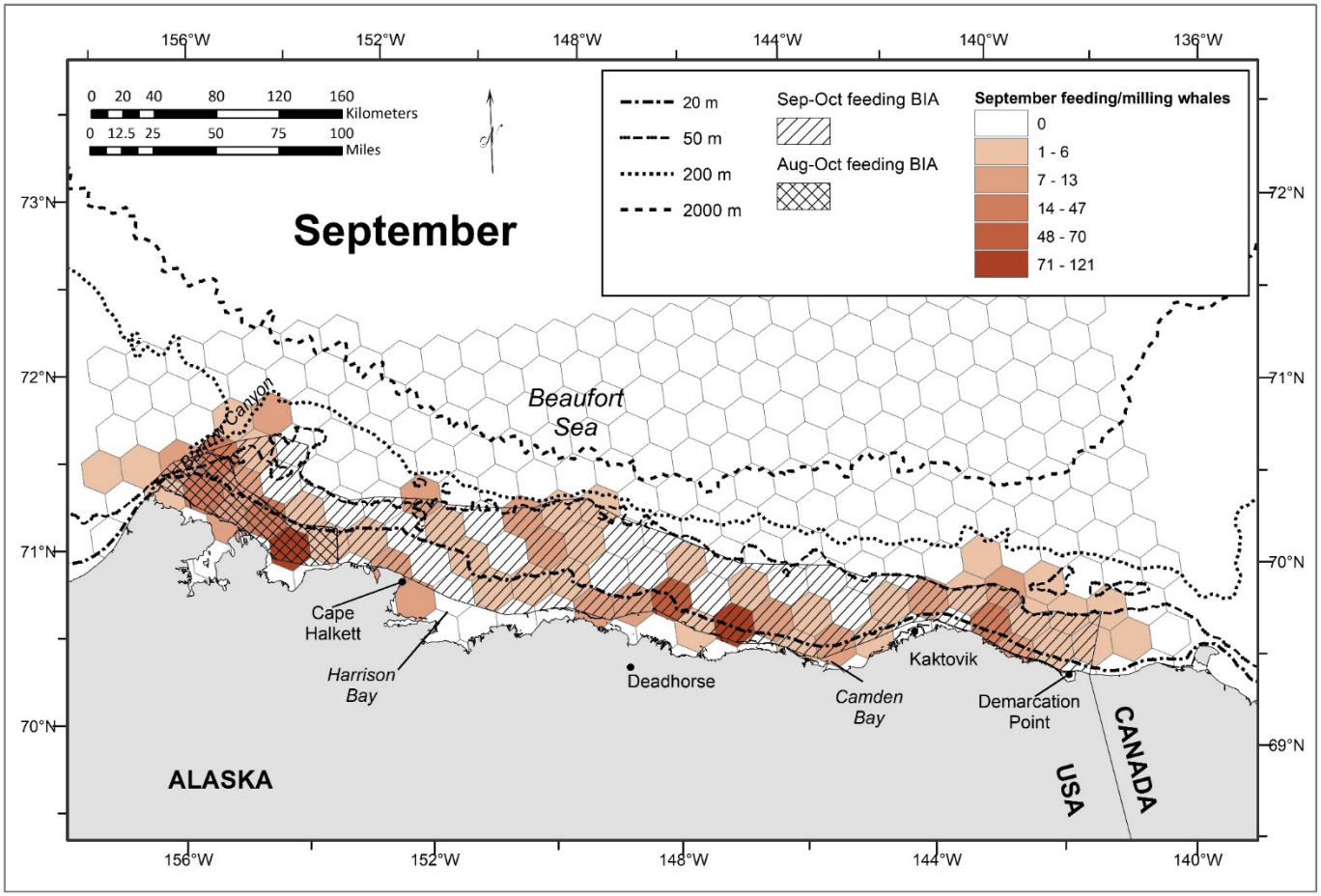

Figure S3C. Number of sightings of feeding and milling bowhead whales during transect and Cetacean Aggregation Protocols passing modes in the western Beaufort Sea during September from 2000 to 2019. Polygons representing the Biologically Important Areas (BIAs) for feeding bowhead whales that were delineated during the initial BIA effort (Clarke et al. 2015) are also shown.

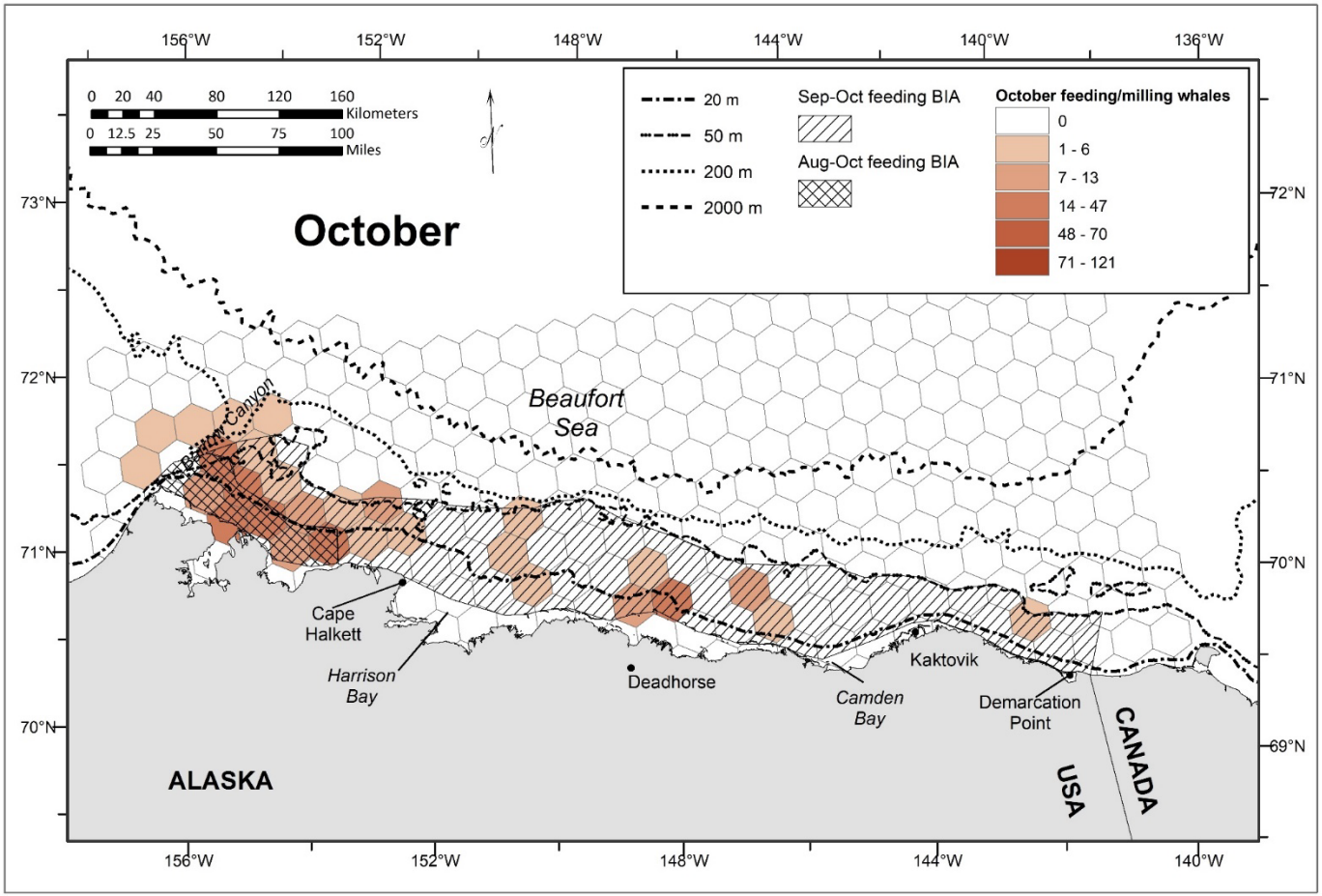

Figure S3D. Number of sightings of feeding and milling bowhead whales during transect and Cetacean Aggregation Protocols passing modes in the western Beaufort Sea during October from 2000 to 2019. Polygons representing the Biologically Important Areas (BIAs) for feeding bowhead whales that were delineated during the initial BIA effort (Clarke et al. 2015) are also shown.

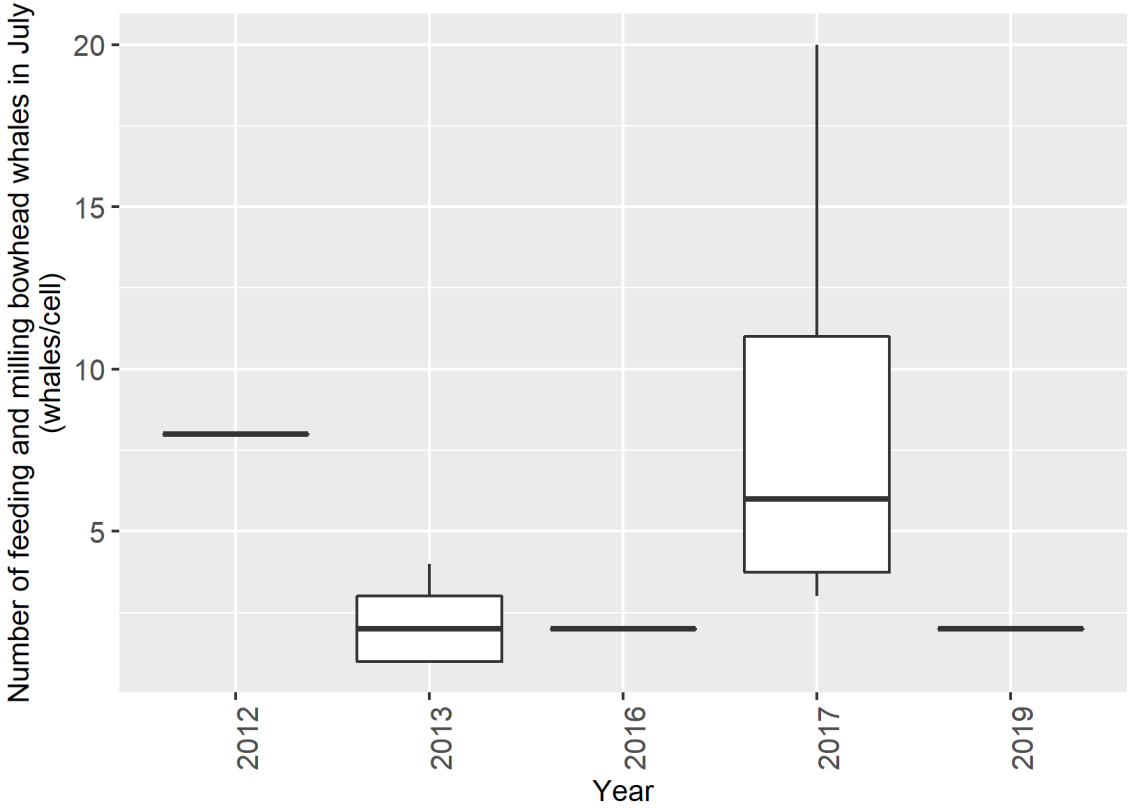

Figure S4A. Distribution of the number of sightings of feeding and milling bowhead whales per hexagonal cell during transect and Cetacean Aggregation Protocols passing modes in the western Beaufort Sea during July of each year from 2000 to 2019. Only cells with at least one feeding/milling bowhead whale sighting were included. For each year, five summary statistics are presented: the median, 25th percentile (lower hinge), 75th percentile (upper hinge), lower whisker, and upper whisker. The lower whisker extends from the hinge to the smallest value at most 1.5 * IQR of the hinge, where IQR is the inter-quartile range, or distance between the 25th and 75th percentiles. The upper whisker extends from the hinge to the largest value no further than 1.5 * IQR from the hinge. Outliers (data beyond the end of the whiskers) are plotted individually.

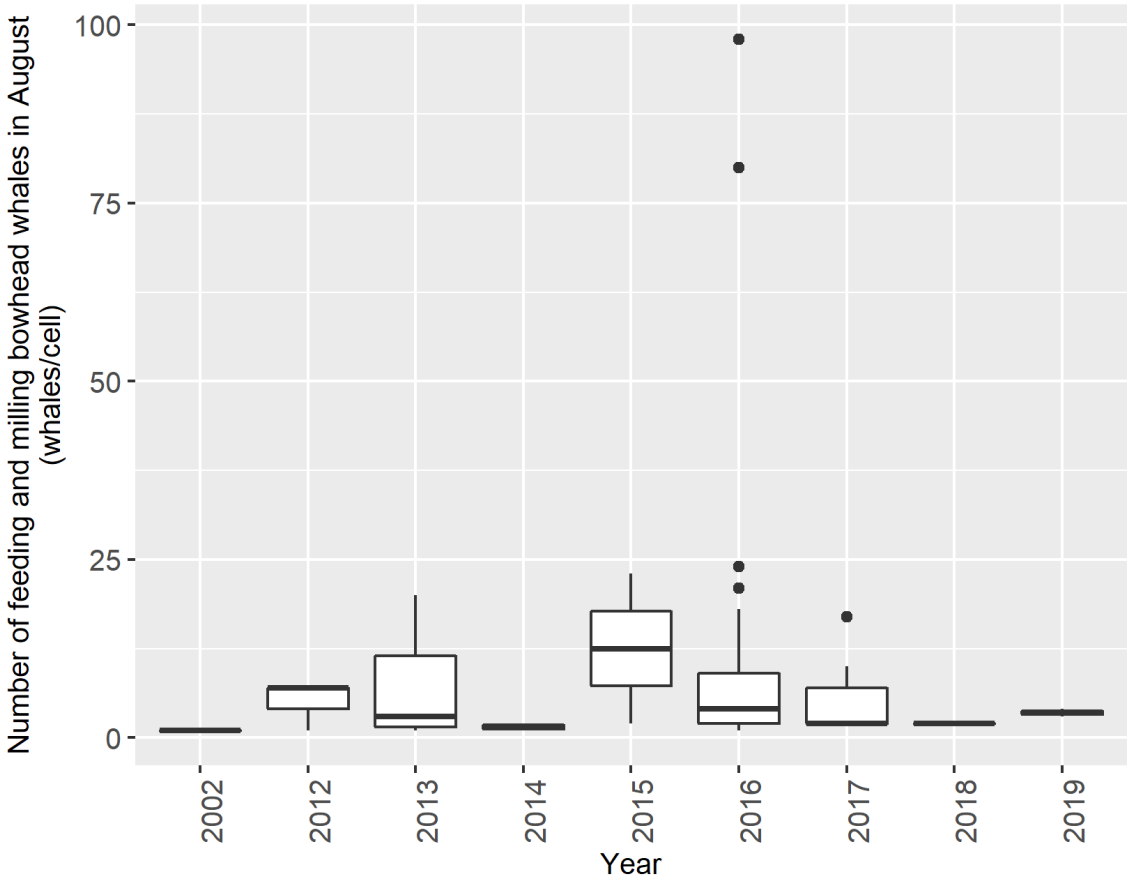

Figure S4B. Distribution of the number of sightings of feeding and milling bowhead whales per hexagonal cell during transect and Cetacean Aggregation Protocols passing modes in the western Beaufort Sea during August of each year from 2000 to 2019. Only cells with at least one feeding/milling bowhead whale sighting were included. For each year, five summary statistics are presented: the median, 25th percentile (lower hinge), 75th percentile (upper hinge), lower whisker, and upper whisker. The lower whisker extends from the hinge to the smallest value at most 1.5 * IQR of the hinge, where IQR is the inter-quartile range, or distance between the 25th and 75th percentiles. The upper whisker extends from the hinge to the largest value no further than 1.5 * IQR from the hinge. Outliers (data beyond the end of the whiskers) are plotted individually.

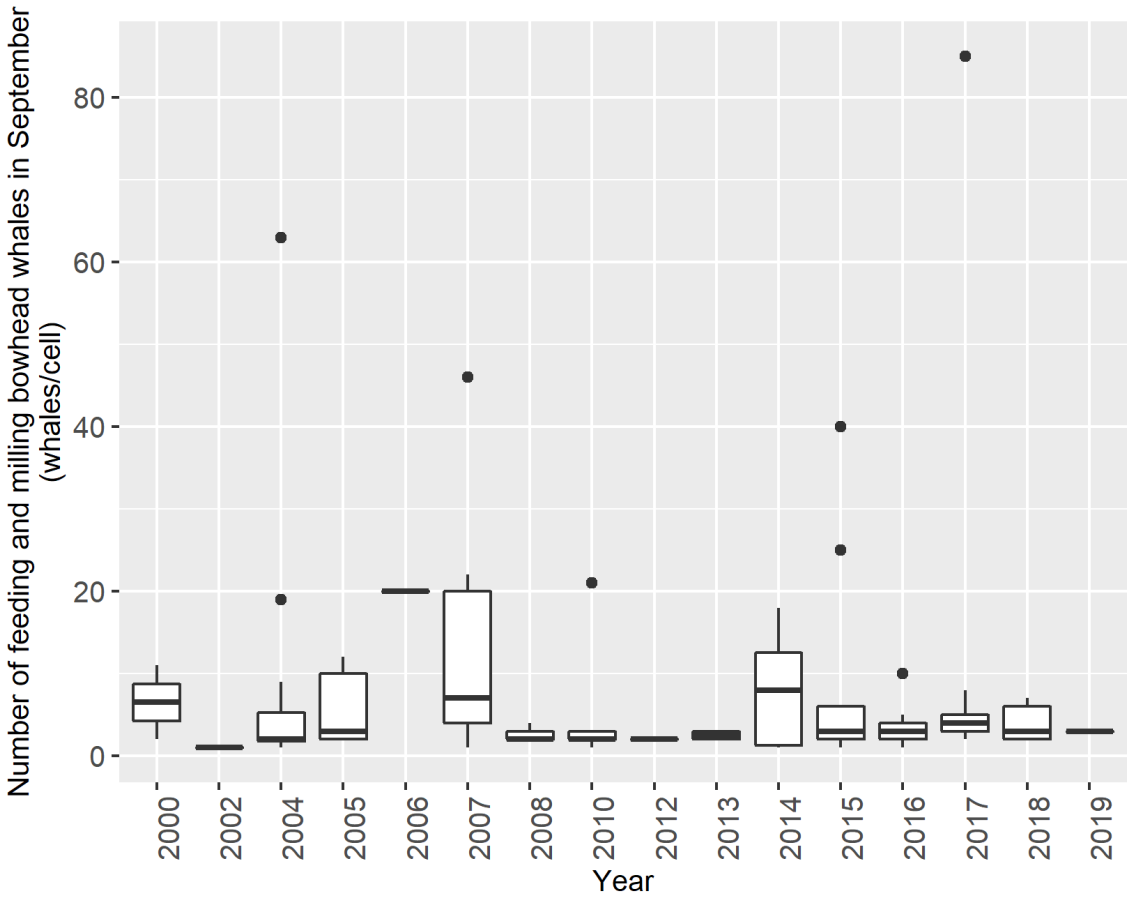

Figure S4C. Distribution of the number of sightings of feeding and milling bowhead whales per hexagonal cell during transect and Cetacean Aggregation Protocols passing modes in the western Beaufort Sea during September of each year from 2000 to 2019. Only cells with at least one feeding/milling bowhead whale sighting were included. For each year, five summary statistics are presented: the median, 25th percentile (lower hinge), 75th percentile (upper hinge), lower whisker, and upper whisker. The lower whisker extends from the hinge to the smallest value at most 1.5 * IQR of the hinge, where IQR is the inter-quartile range, or distance between the 25th and 75th percentiles. The upper whisker extends from the hinge to the largest value no further than 1.5 * IQR from the hinge. Outliers (data beyond the end of the whiskers) are plotted individually.

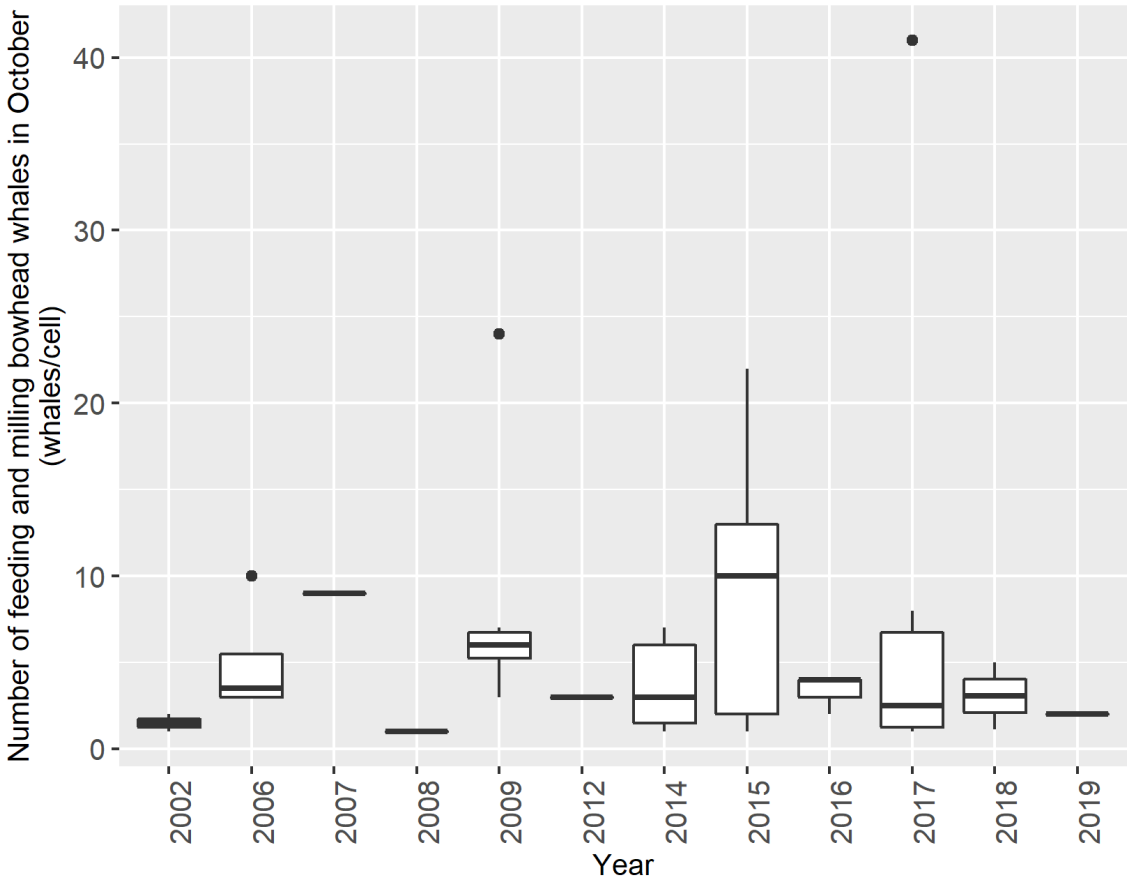

Figure S4D. Distribution of the number of sightings of feeding and milling bowhead whales per hexagonal cell during transect and Cetacean Aggregation Protocols passing modes in the western Beaufort Sea during October of each year from 2000 to 2019. Only cells with at least one feeding/milling bowhead whale sighting were included. For each year, five summary statistics are presented: the median, 25th percentile (lower hinge), 75th percentile (upper hinge), lower whisker, and upper whisker. The lower whisker extends from the hinge to the smallest value at most 1.5 * IQR of the hinge, where IQR is the inter-quartile range, or distance between the 25th and 75th percentiles. The upper whisker extends from the hinge to the largest value no further than 1.5 * IQR from the hinge. Outliers (data beyond the end of the whiskers) are plotted individually.

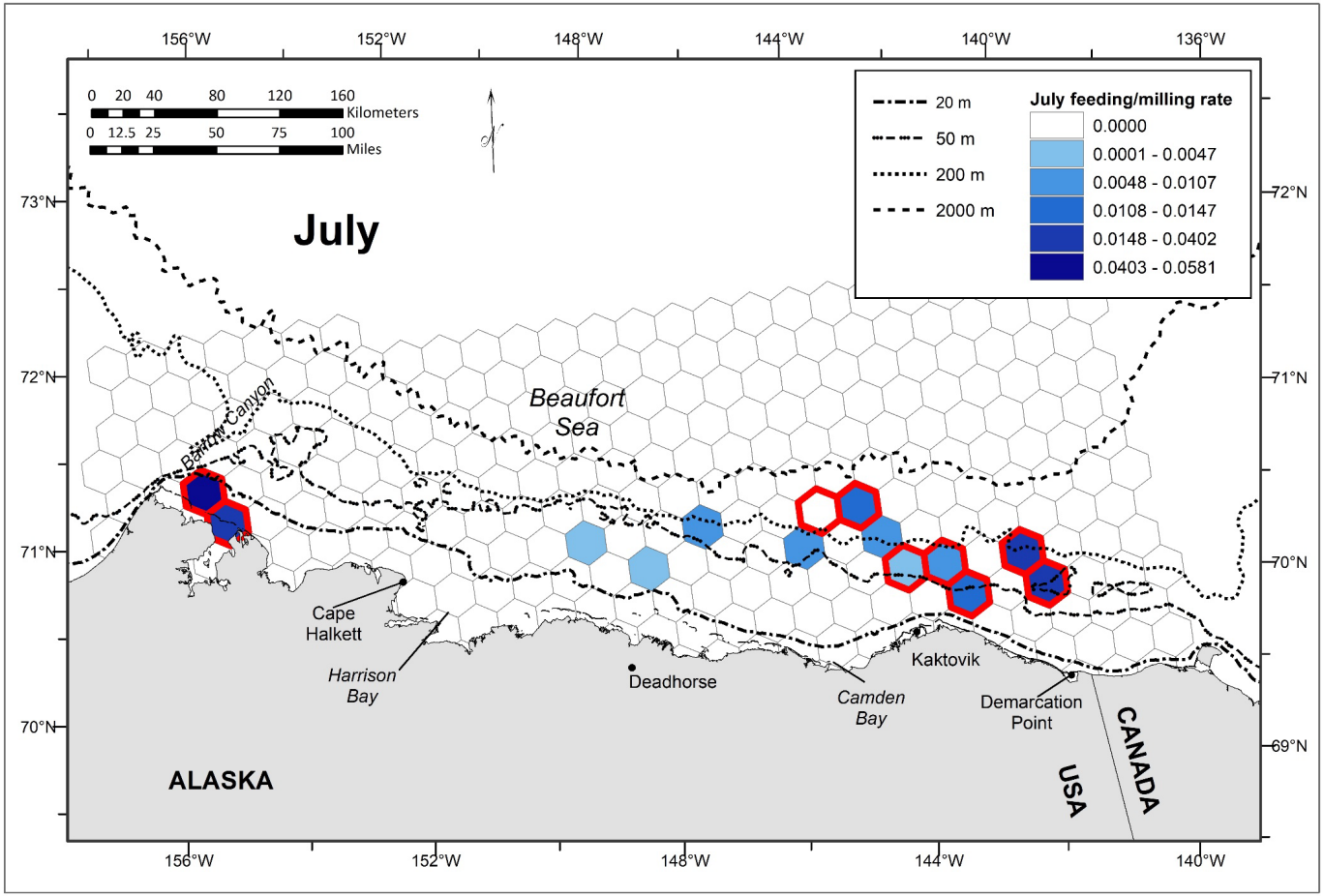

Figure S5A. Rate of feeding or milling bowhead whale sightings (# whales/km) during transect and Cetacean Aggregation Protocols passing modes in the western Beaufort Sea during July from 2000 to 2019. Red outlines surround cells chosen as the selected BIA scenarios based on the proposed optimization model results.

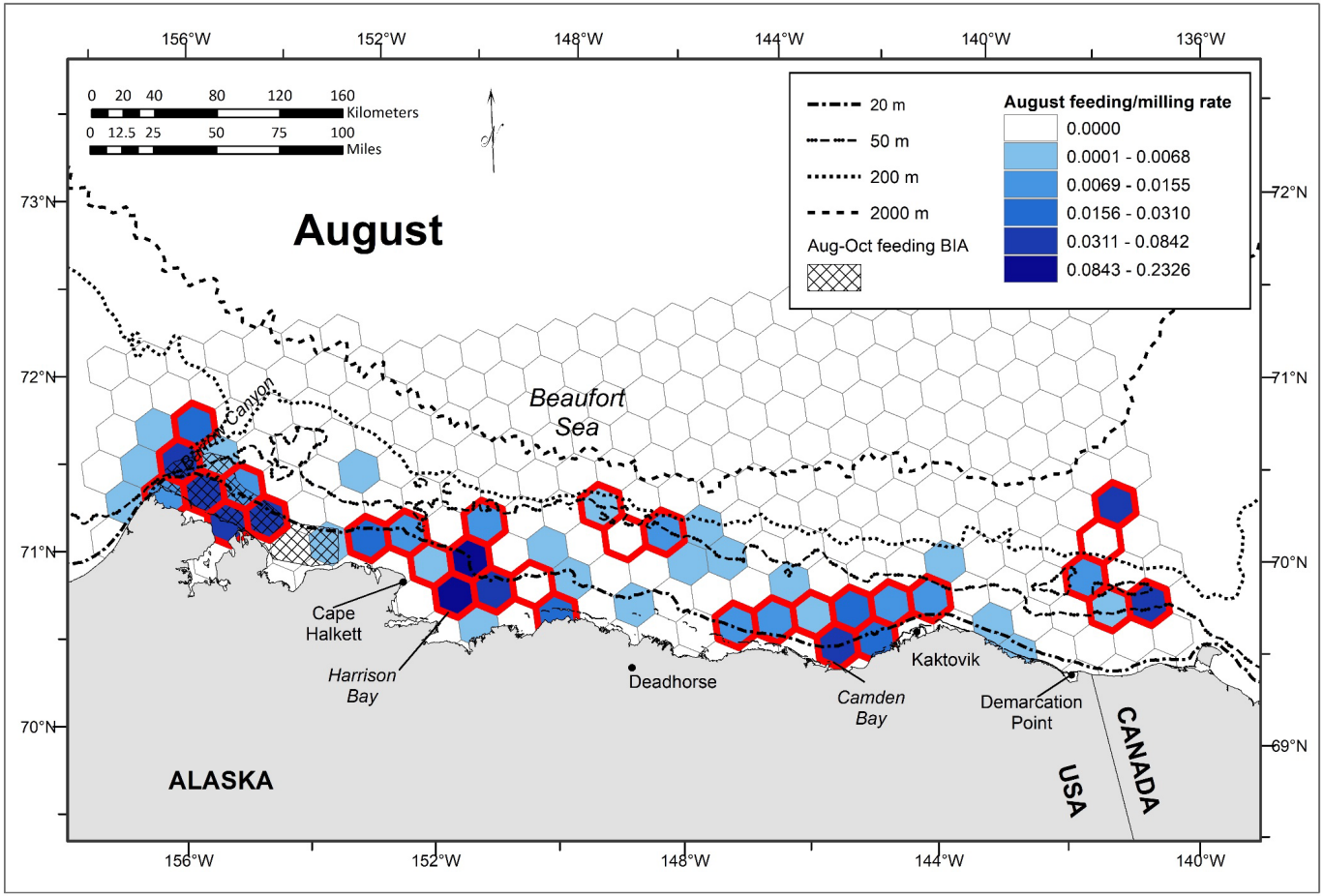

Figure S5B. Rate of feeding or milling bowhead whale sightings (# whales/km) during transect and Cetacean Aggregation Protocols passing modes in the western Beaufort Sea during August from 2000 to 2019. Polygons with crosshatched shading represent the old Biologically Important Areas (BIAs) for feeding bowhead whales that were delineated during the first BIA effort (Clarke et al. 2015). Red outlines surround cells chosen as the selected BIA scenarios based on the proposed optimization model results.

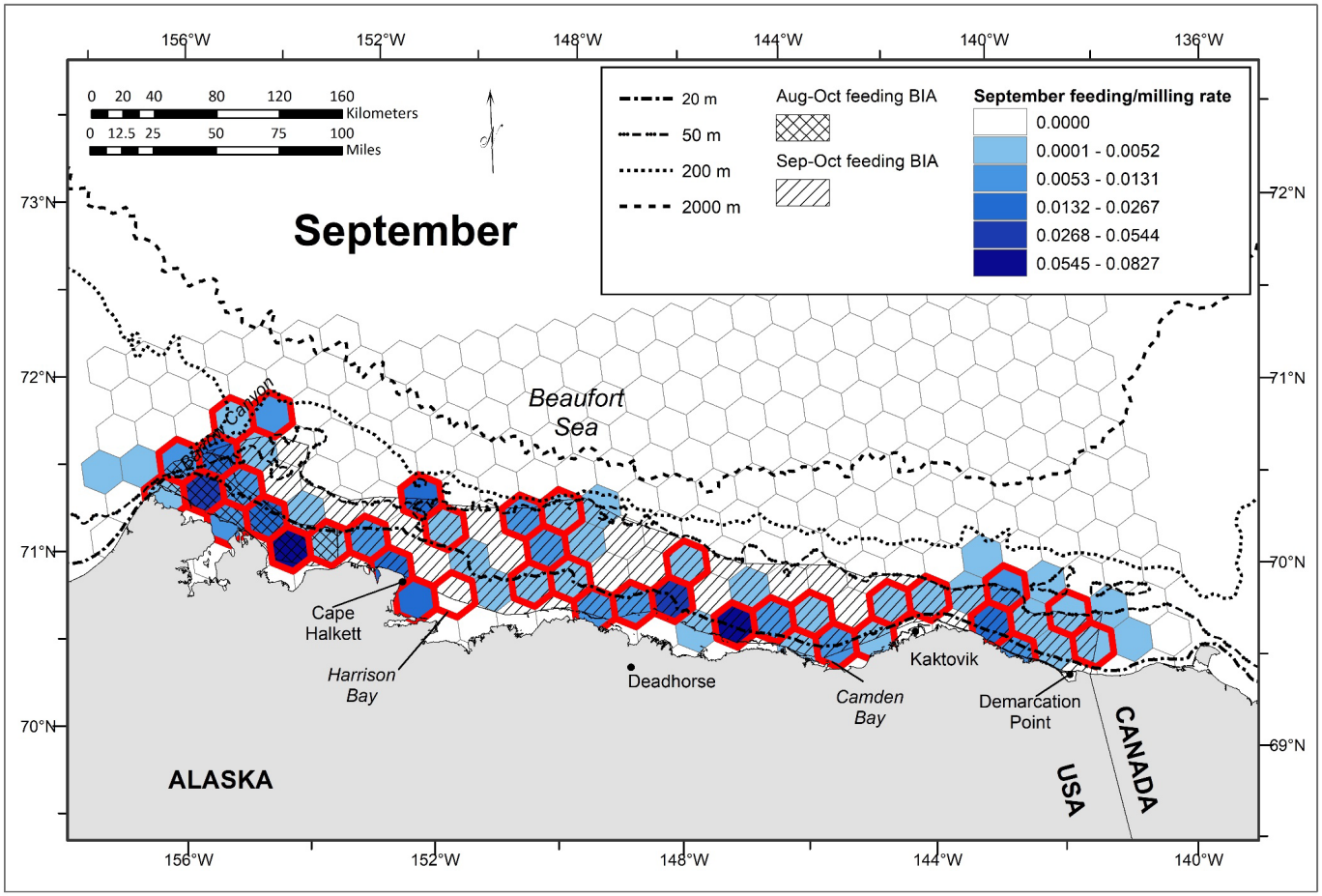

Figure S5C. Rate of feeding or milling bowhead whale sightings (# whales/km) during transect and Cetacean Aggregation Protocols passing modes in the western Beaufort Sea during September from 2000 to 2019. Polygons with crosshatched shading represent the old Biologically Important Areas (BIAs) for feeding bowhead whales that were delineated during the first BIA effort (Clarke et al. 2015). Red outlines surround cells chosen as the selected BIA scenarios based on the proposed optimization model results.

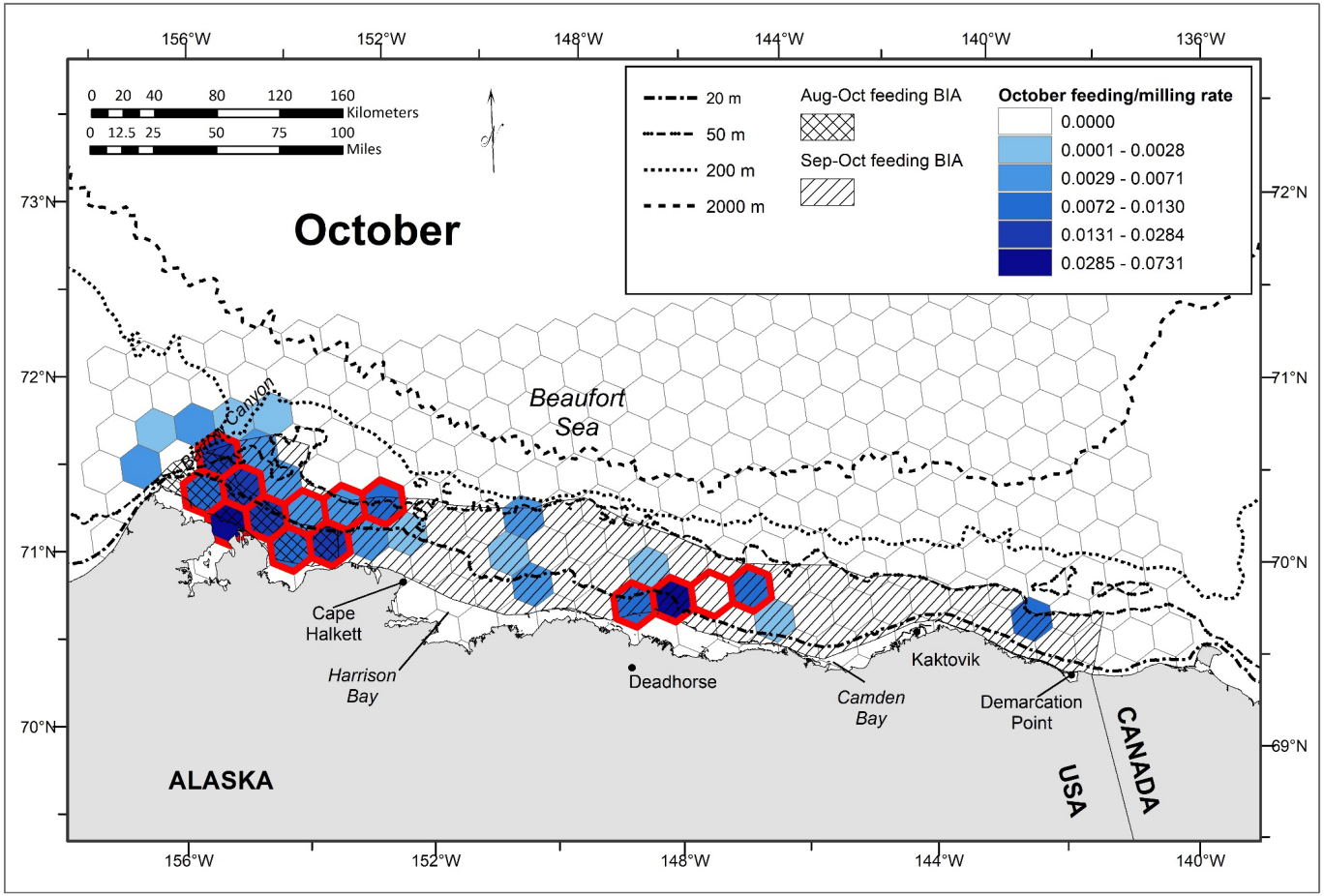

Figure S5D. Rate of feeding or milling bowhead whale sightings (# whales/km) during transect and Cetacean Aggregation Protocols passing modes in the western Beaufort Sea during October from 2000 to 2019. Polygons with crosshatched shading represent the old Biologically Important Areas (BIAs) for feeding bowhead whales that were delineated during the first BIA effort (Clarke et al. 2015). Red outlines surround cells chosen as the selected BIA scenarios based on the proposed optimization model results.

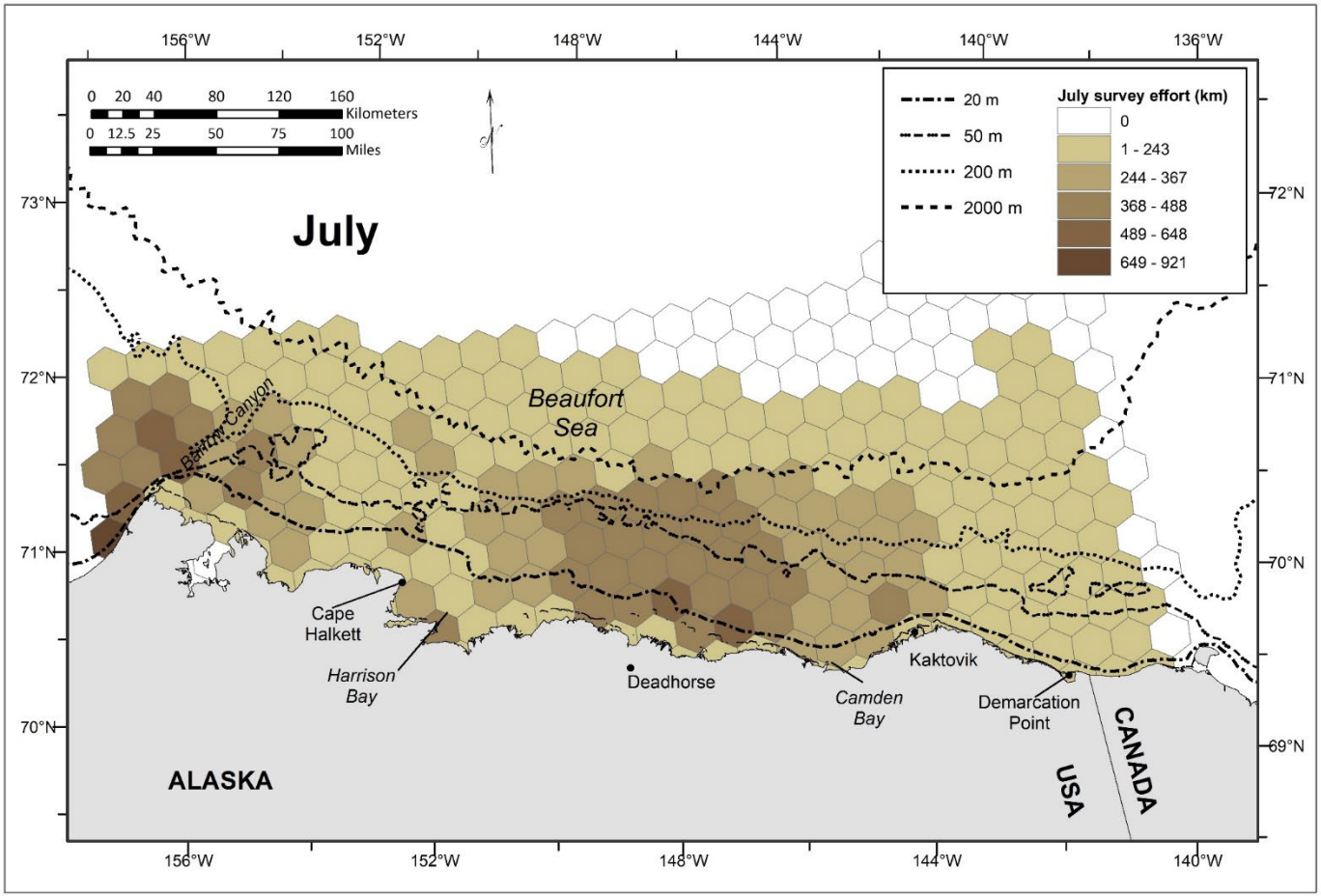

Figure S6A. July aerial survey effort (transect and Cetacean Aggregation Protocols passing modes) in the western Beaufort Sea, pooled across years 2012-2019.

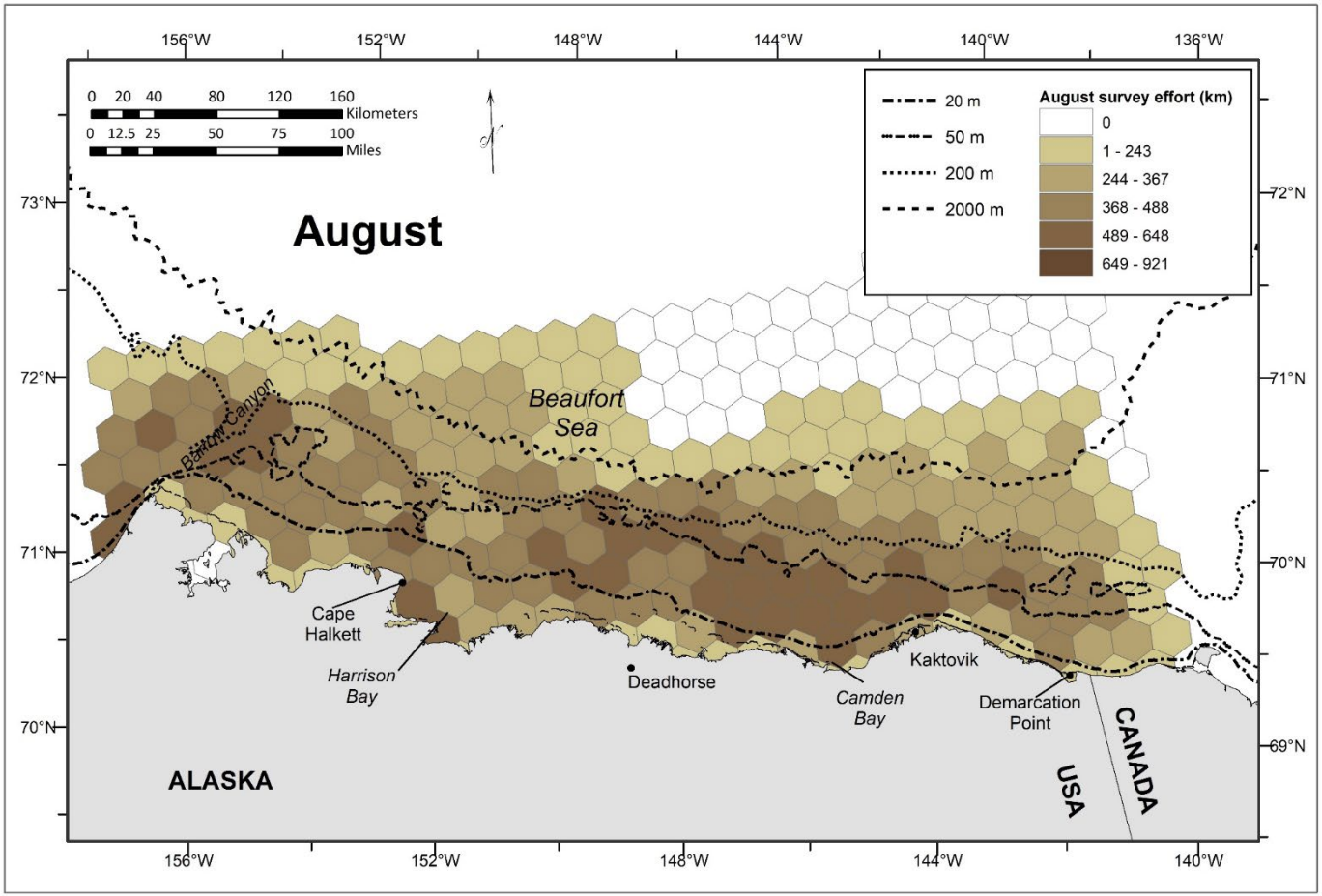

Figure S6B. August aerial survey effort (transect and Cetacean Aggregation Protocols passing modes) in the western Beaufort Sea, pooled across years 2012-2019.

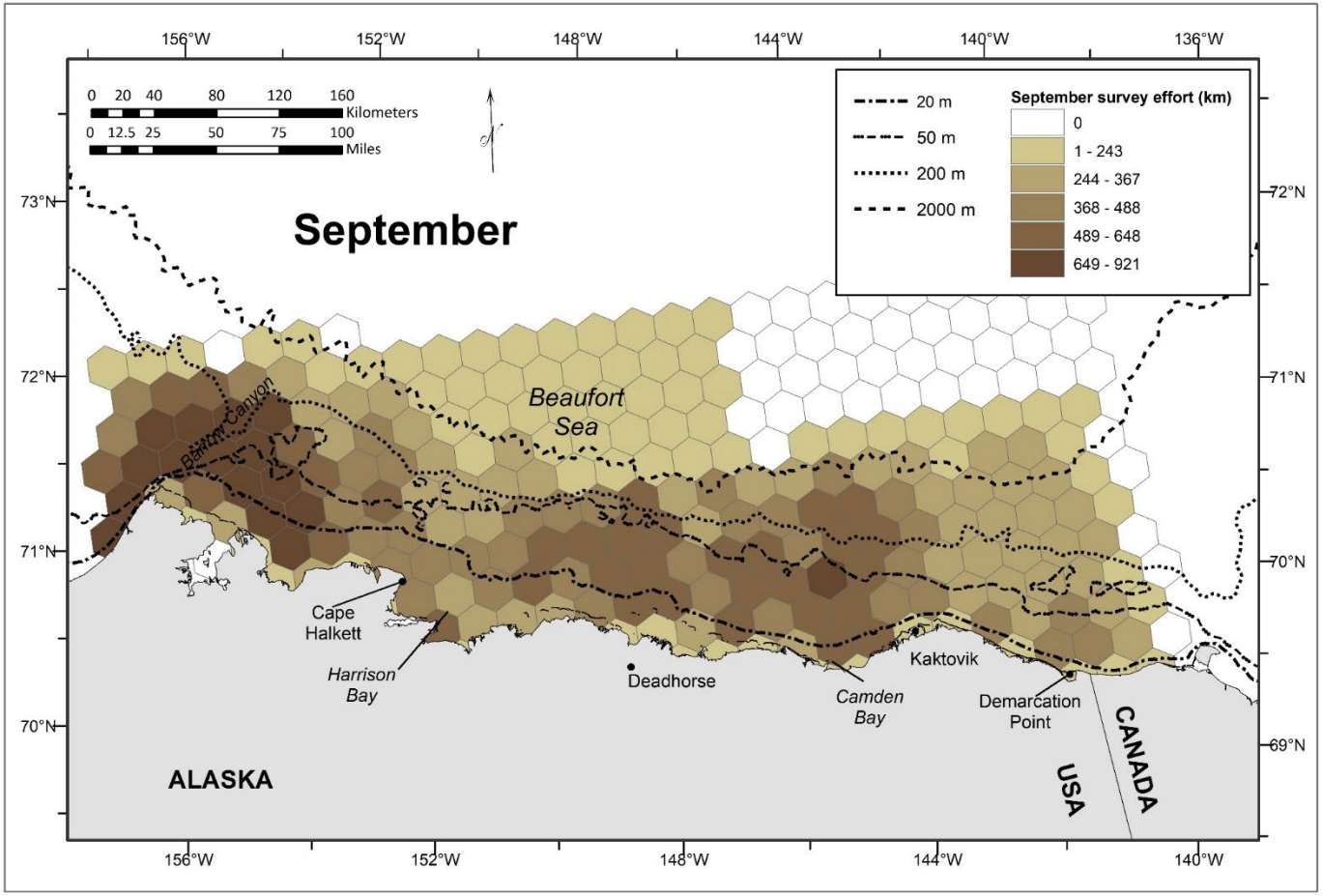

Figure S6C. September aerial survey effort (transect and Cetacean Aggregation Protocols passing modes) in the western Beaufort Sea, pooled across years 2012-2019.

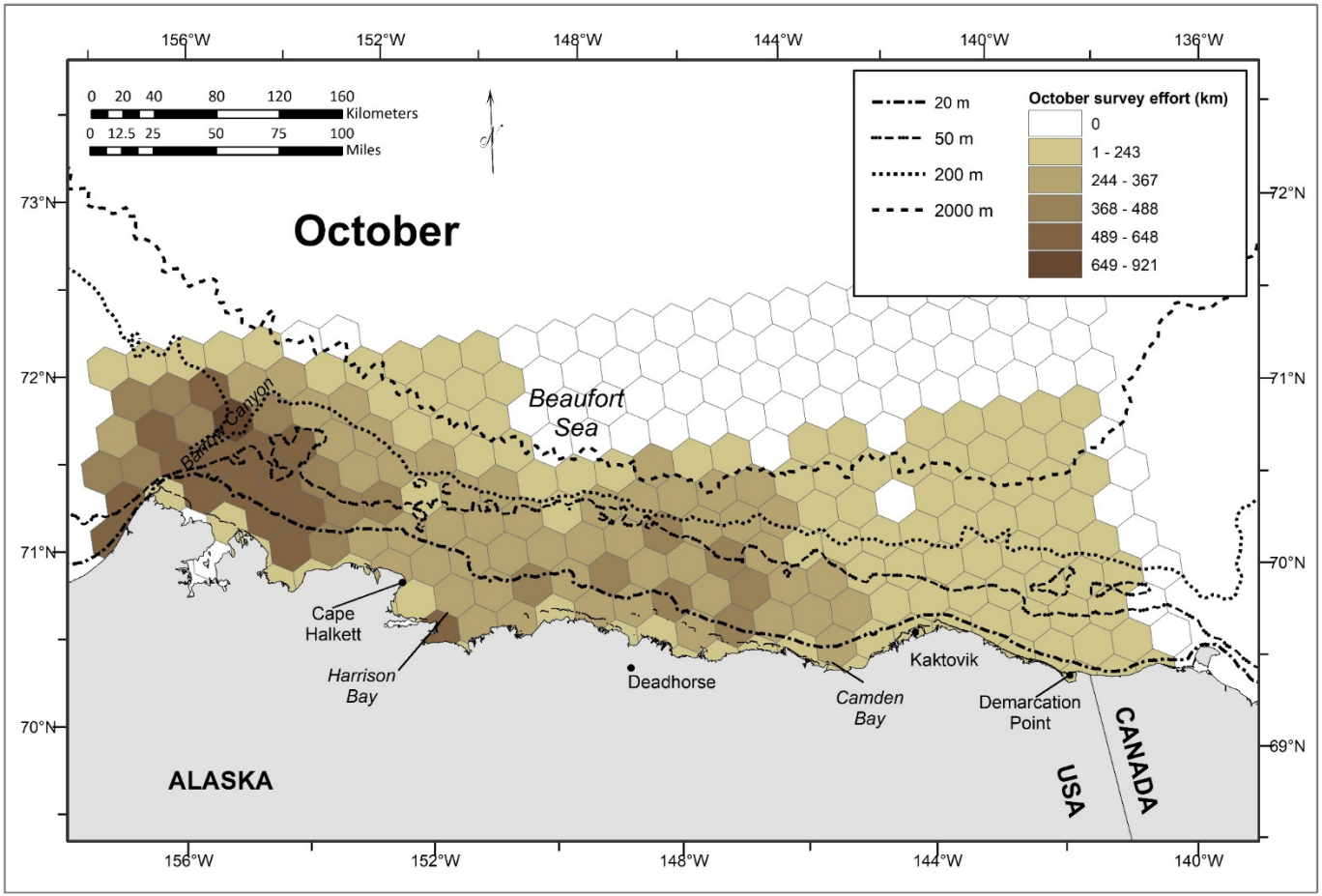

Figure S6D. October aerial survey effort (transect and Cetacean Aggregation Protocols passing modes) in the western Beaufort Sea, pooled across years 2012-2019.

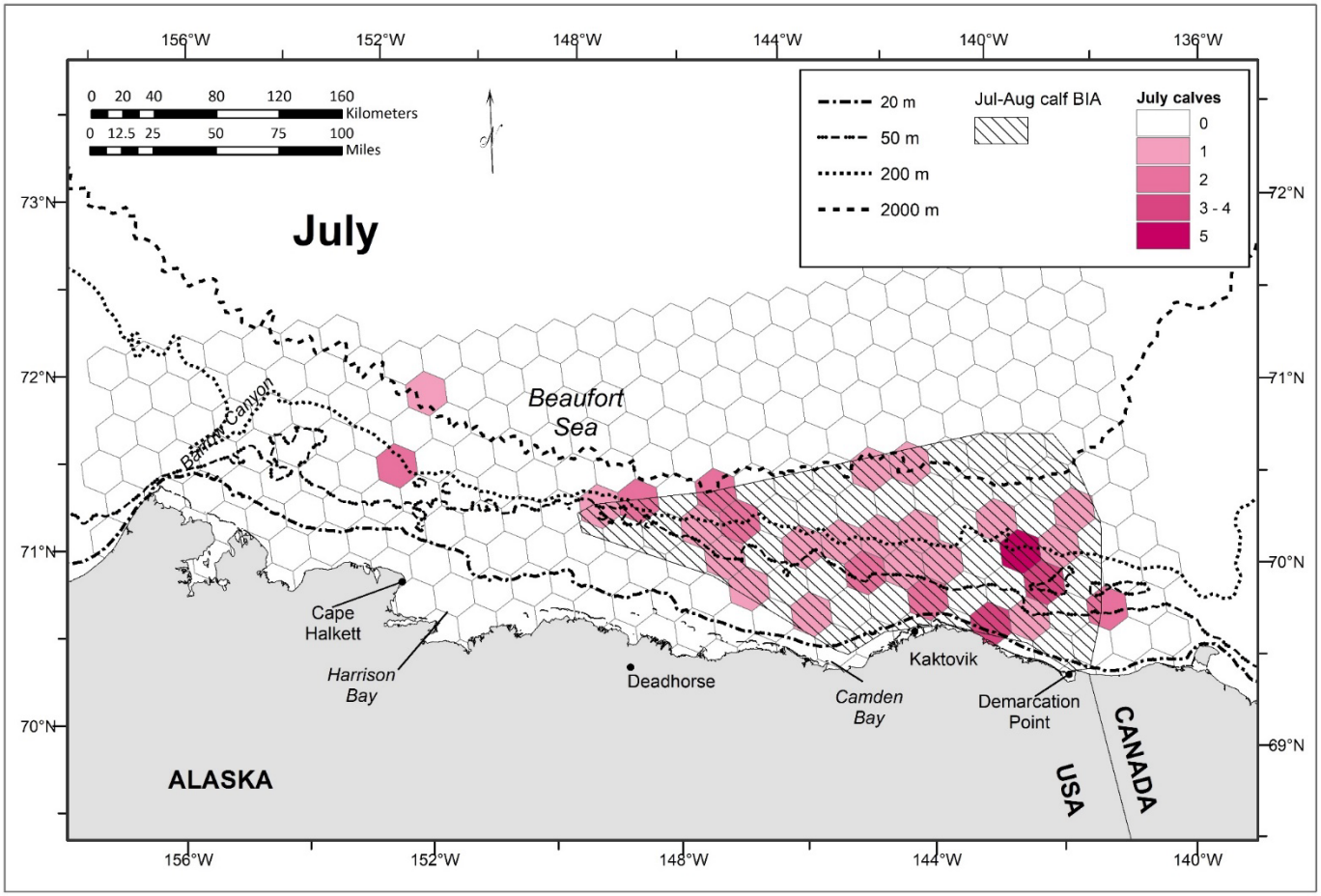

Figure S7A. Number of sightings of bowhead whale calves during transect and Cetacean Aggregation Protocols passing modes in the western Beaufort Sea during July from 2012 to 2019. Polygons representing the Biologically Important Areas (BIAs) for bowhead whale calves that were delineated during the initial BIA effort (Clarke et al. 2015) are also shown.

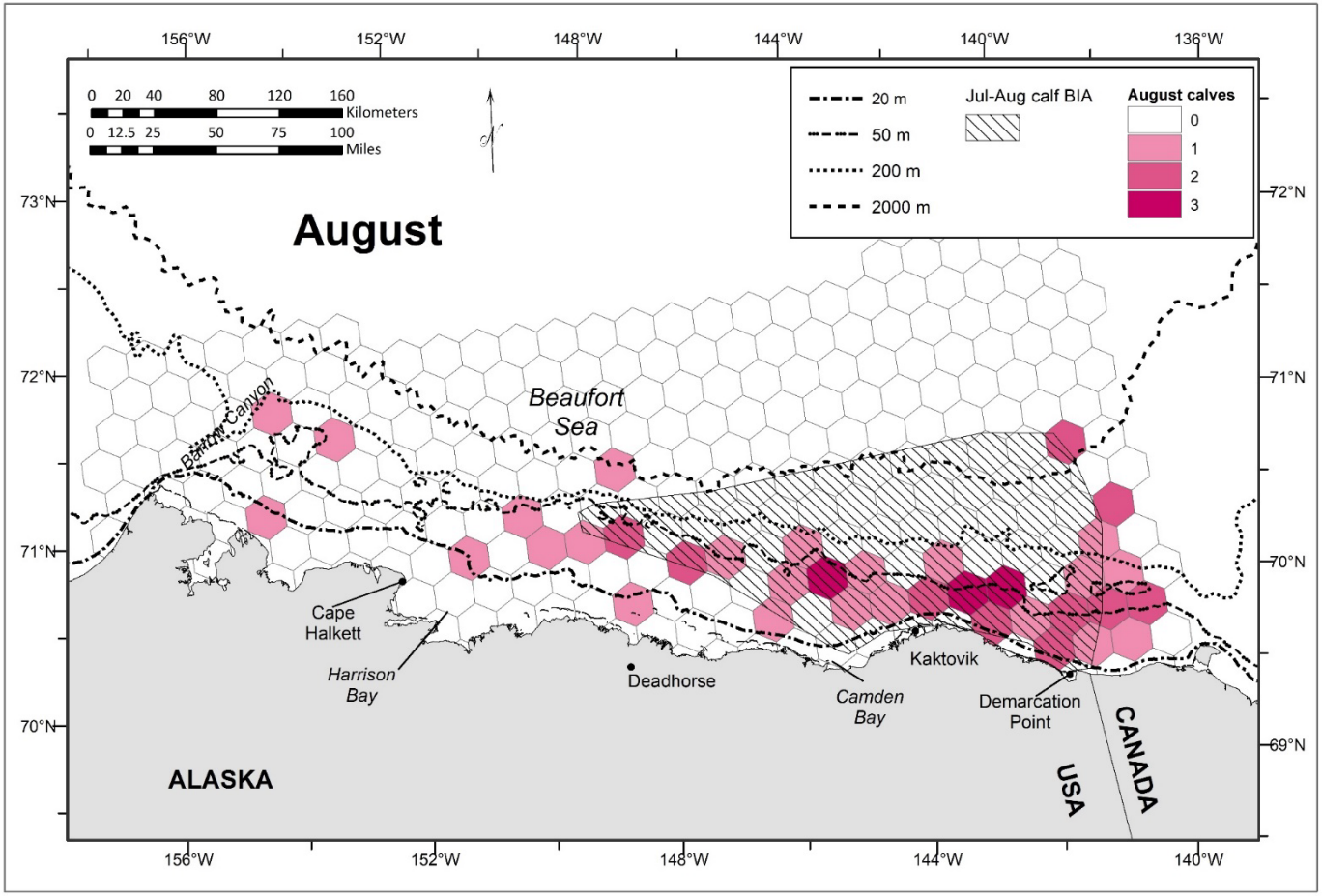

Figure S7B. Number of sightings of bowhead whale calves during transect and Cetacean Aggregation Protocols passing modes in the western Beaufort Sea during August from 2012 to 2019. Polygons representing the Biologically Important Areas (BIAs) for bowhead whale calves that were delineated during the initial BIA effort (Clarke et al. 2015) are also shown.

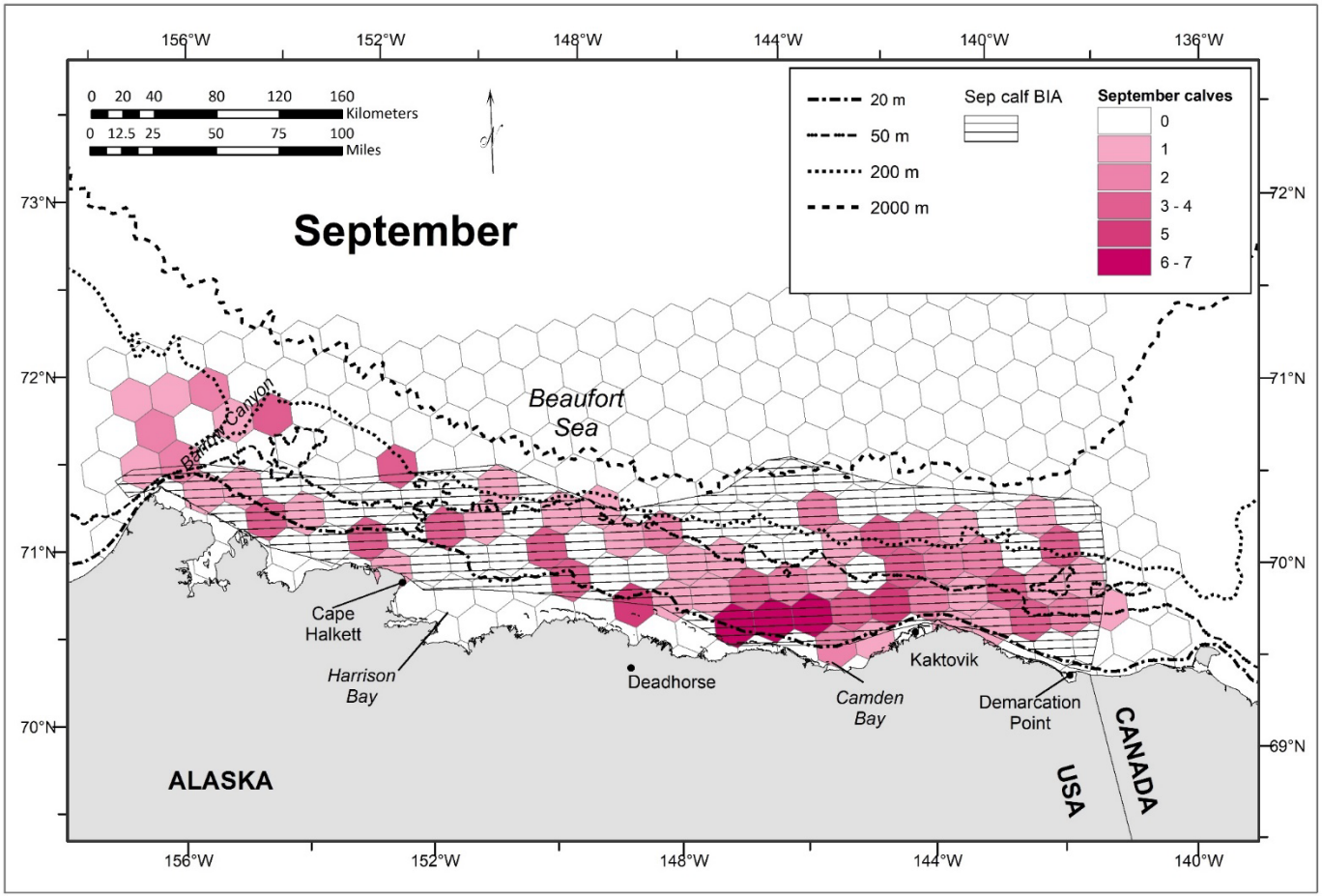

Figure S7C. Number of sightings of bowhead whale calves during transect and Cetacean Aggregation Protocols passing modes in the western Beaufort Sea during September from 2012 to 2019. Polygons representing the Biologically Important Areas (BIAs) for bowhead whale calves that were delineated during the initial BIA effort (Clarke et al. 2015) are also shown.

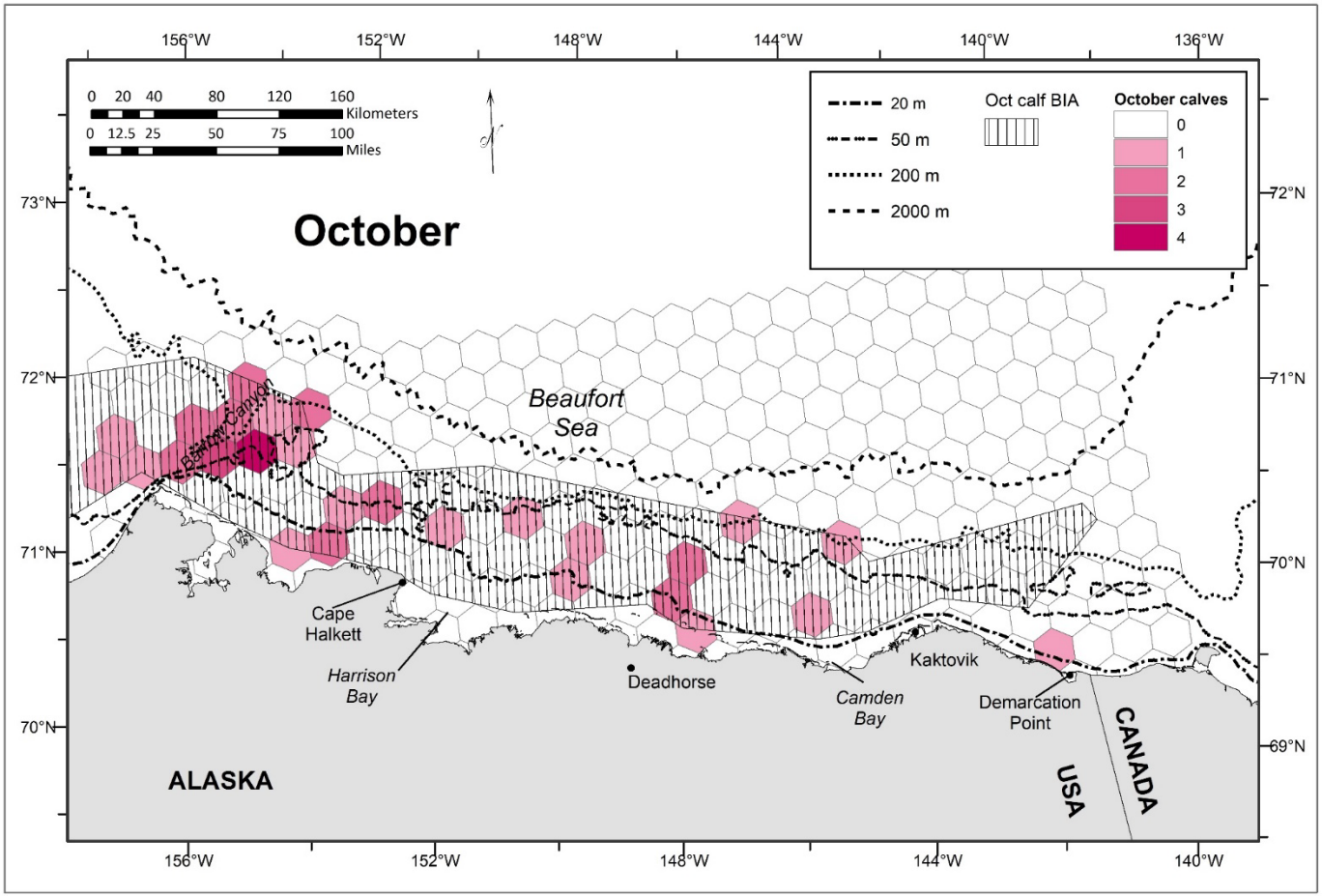

Figure S7D. Number of sightings of bowhead whale calves during transect and Cetacean Aggregation Protocols passing modes in the western Beaufort Sea during October from 2012 to 2019. Polygons representing the Biologically Important Areas (BIAs) for bowhead whale calves that were delineated during the initial BIA effort (Clarke et al. 2015) are also shown.

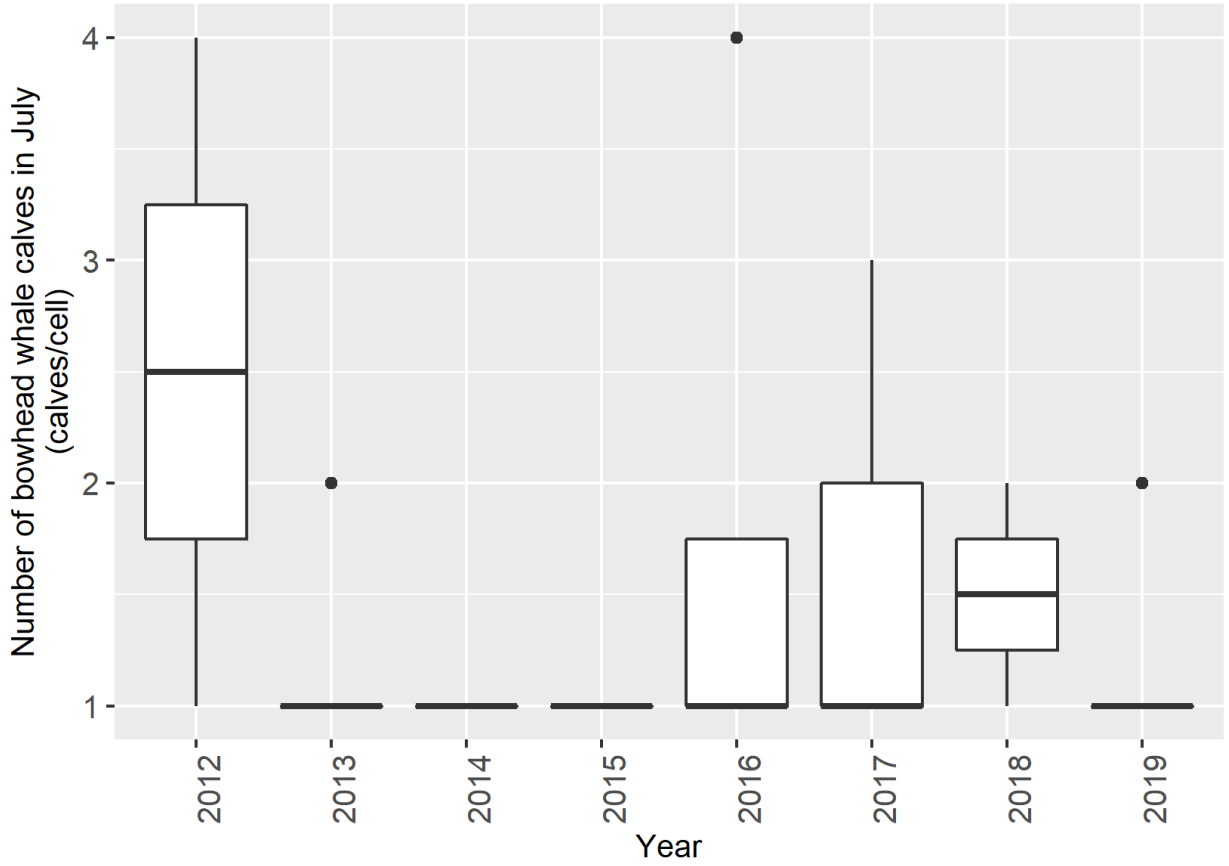

Figure S8A. Distribution of the number of sightings of bowhead whale calves per hexagonal cell during transect and Cetacean Aggregation Protocols passing modes in the western Beaufort Sea during July from 2012 to 2019. Only cells with at least one bowhead whale calf sighting were included. For each year, five summary statistics are presented: the median, 25th percentile (lower hinge), 75th percentile (upper hinge), lower whisker, and upper whisker. The lower whisker extends from the hinge to the smallest value at most 1.5 * IQR of the hinge, where IQR is the inter-quartile range, or distance between the 25th and 75th percentiles. The upper whisker extends from the hinge to the largest value no further than 1.5 * IQR from the hinge. Outliers (data beyond the end of the whiskers) are plotted individually.

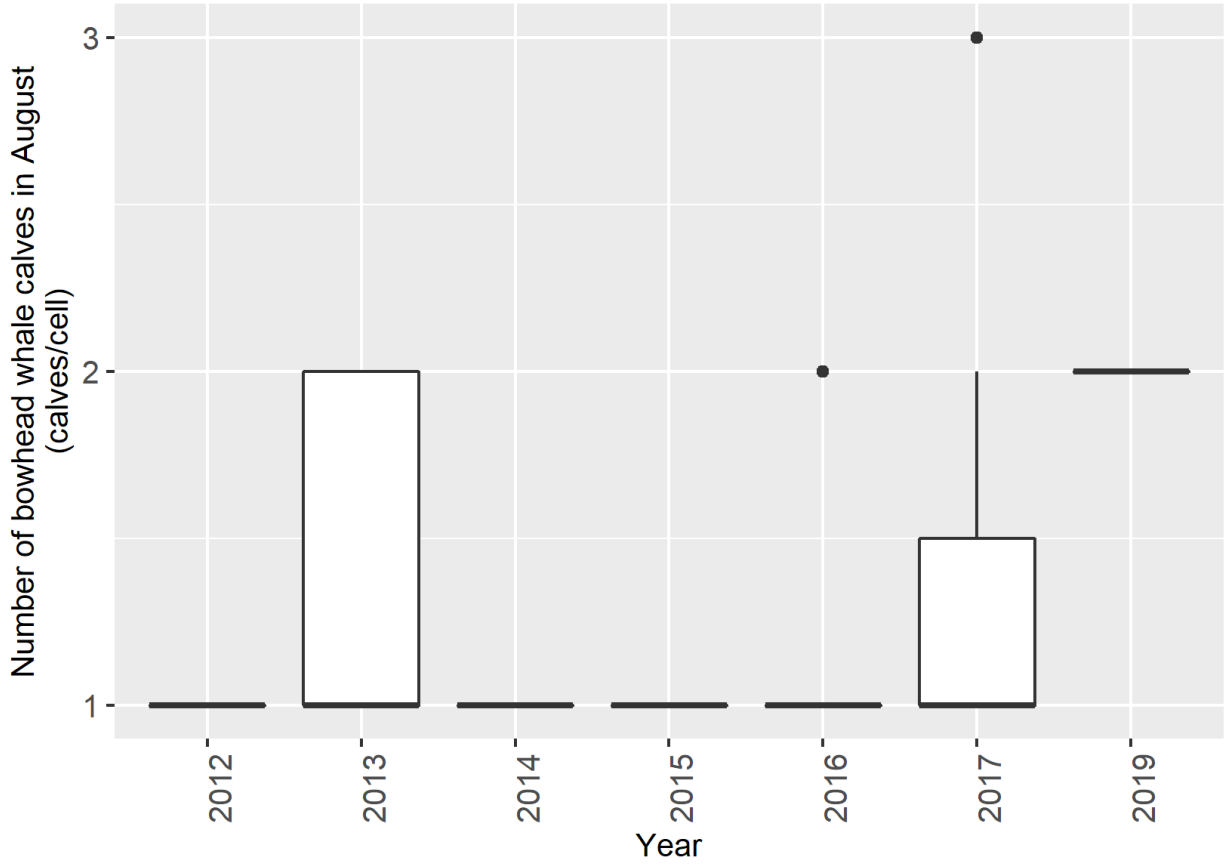

Figure S8B. Distribution of the number of sightings of bowhead whale calves per hexagonal cell during transect and Cetacean Aggregation Protocols passing modes in the western Beaufort Sea during August from 2012 to 2019. Only cells with at least one bowhead whale calf sighting were included. For each year, five summary statistics are presented: the median, 25th percentile (lower hinge), 75th percentile (upper hinge), lower whisker, and upper whisker. The lower whisker extends from the hinge to the smallest value at most 1.5 * IQR of the hinge, where IQR is the inter-quartile range, or distance between the 25th and 75th percentiles. The upper whisker extends from the hinge to the largest value no further than 1.5 * IQR from the hinge. Outliers (data beyond the end of the whiskers) are plotted individually.

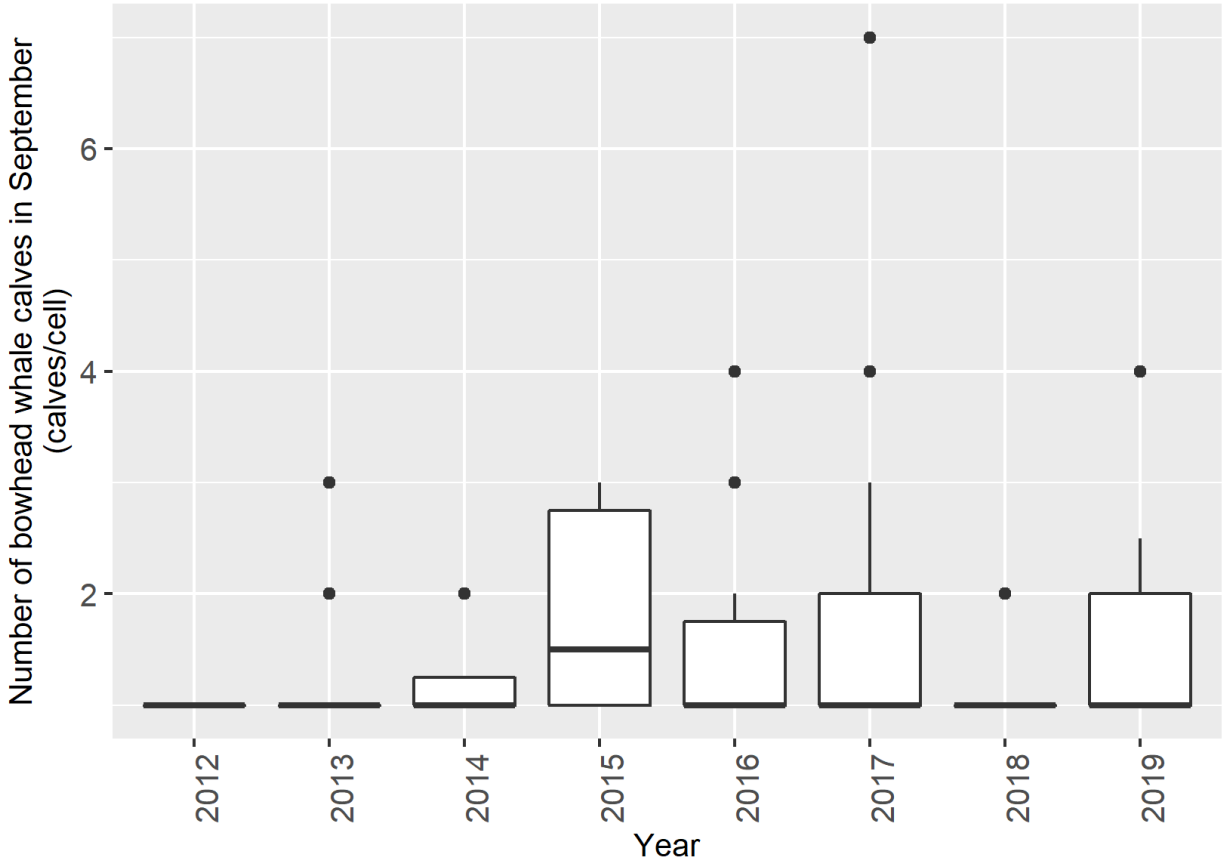

Figure S8C. Distribution of the number of sightings of bowhead whale calves per hexagonal cell during transect and Cetacean Aggregation Protocols passing modes in the western Beaufort Sea during September from 2012 to 2019. Only cells with at least one bowhead whale calf sighting were included. For each year, five summary statistics are presented: the median, 25th percentile (lower hinge), 75th percentile (upper hinge), lower whisker, and upper whisker. The lower whisker extends from the hinge to the smallest value at most 1.5 * IQR of the hinge, where IQR is the inter-quartile range, or distance between the 25th and 75th percentiles. The upper whisker extends from the hinge to the largest value no further than 1.5 * IQR from the hinge. Outliers (data beyond the end of the whiskers) are plotted individually.

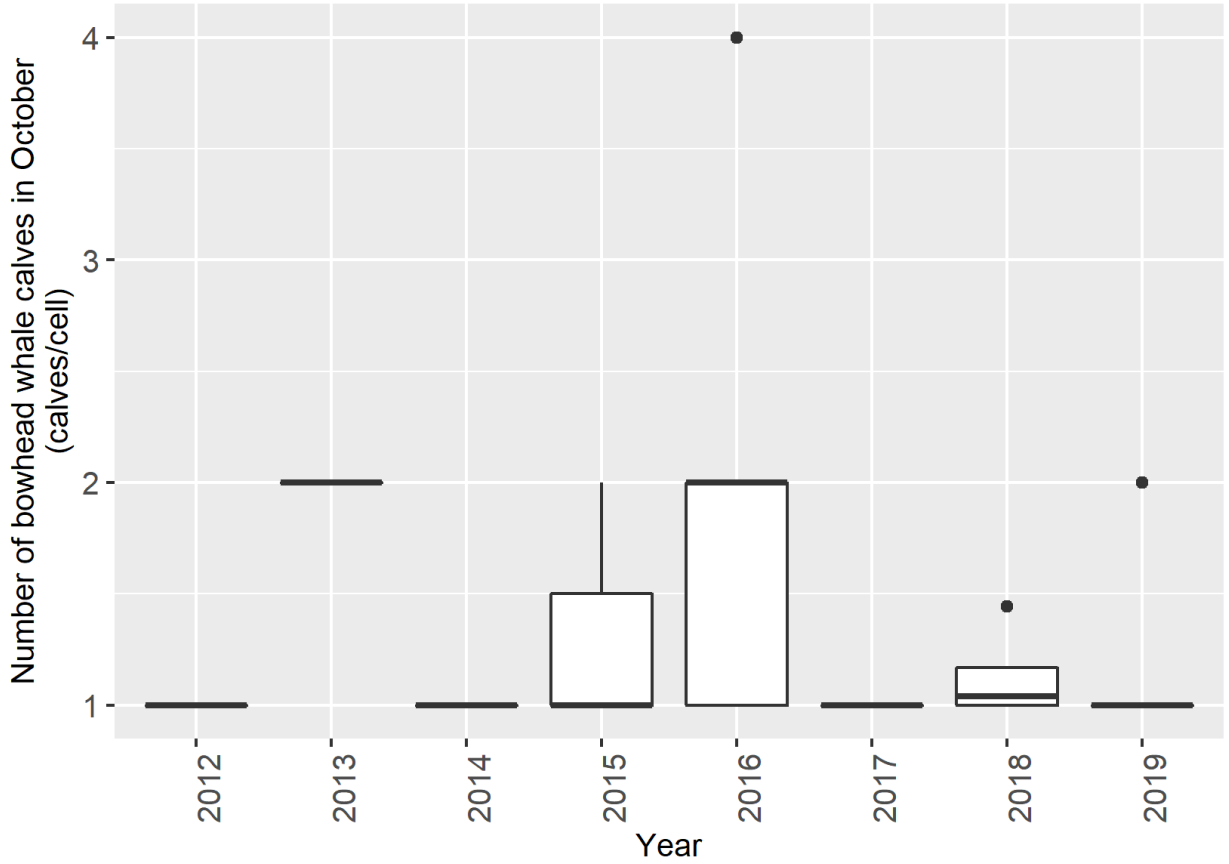

Figure S8D. Distribution of the number of sightings of bowhead whale calves per hexagonal cell during transect and Cetacean Aggregation Protocols passing modes in the western Beaufort Sea during October from 2012 to 2019. Only cells with at least one bowhead whale calf sighting were included. For each year, five summary statistics are presented: the median, 25th percentile (lower hinge), 75th percentile (upper hinge), lower whisker, and upper whisker. The lower whisker extends from the hinge to the smallest value at most 1.5 * IQR of the hinge, where IQR is the inter-quartile range, or distance between the 25th and 75th percentiles. The upper whisker extends from the hinge to the largest value no further than 1.5 * IQR from the hinge. Outliers (data beyond the end of the whiskers) are plotted individually.

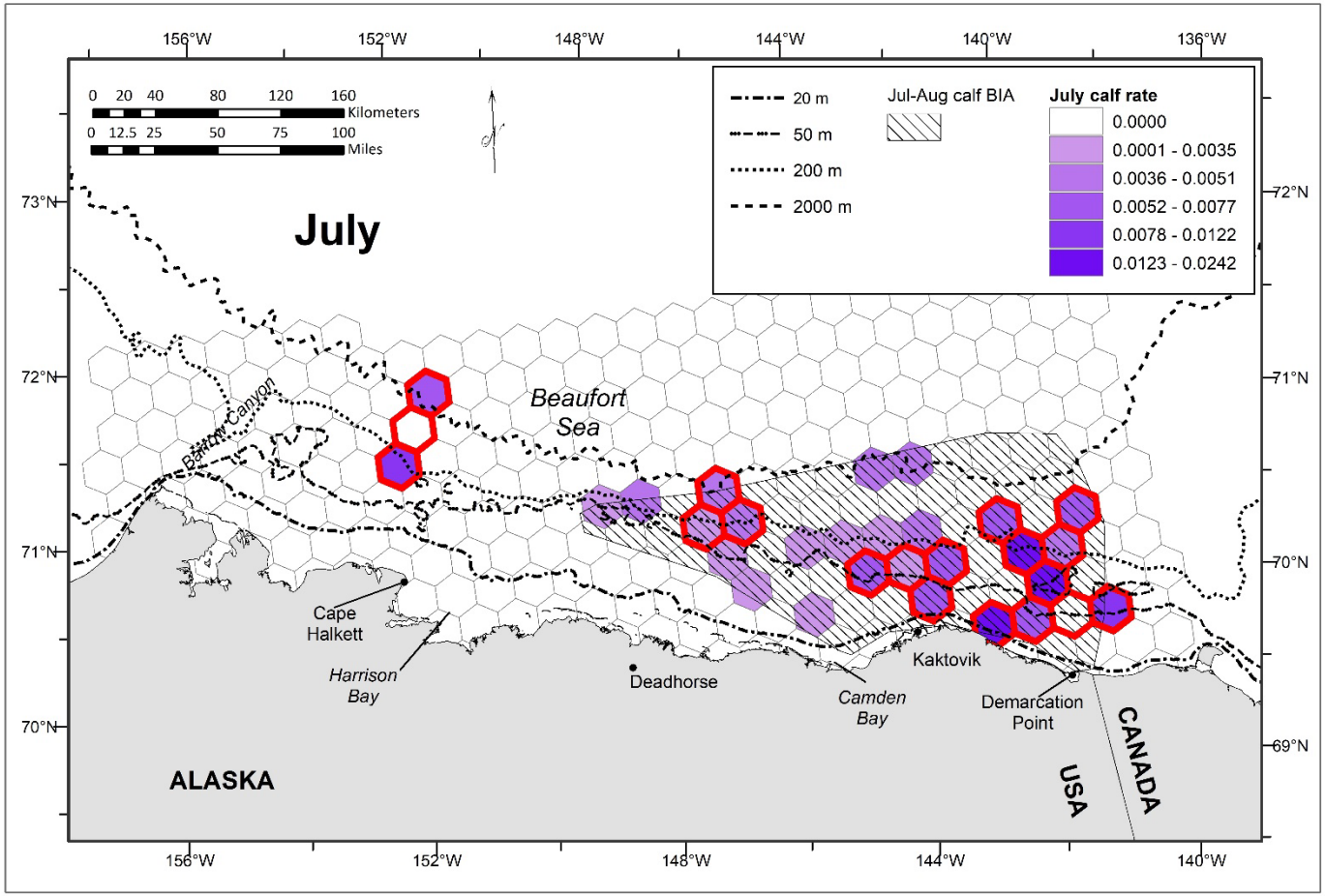

Figure S9A. Bowhead whale calf sighting rate (# calves/km) during transect and Cetacean Aggregation Protocols passing modes in the western Beaufort Sea during July from 2012 to 2019. Polygons with crosshatched shading represent the old Biologically Important Areas (BIAs) for bowhead whale calves that were delineated during the first BIA effort (Clarke et al. 2015). Red outlines surround cells chosen as the selected BIA scenarios based on the proposed optimization model results.

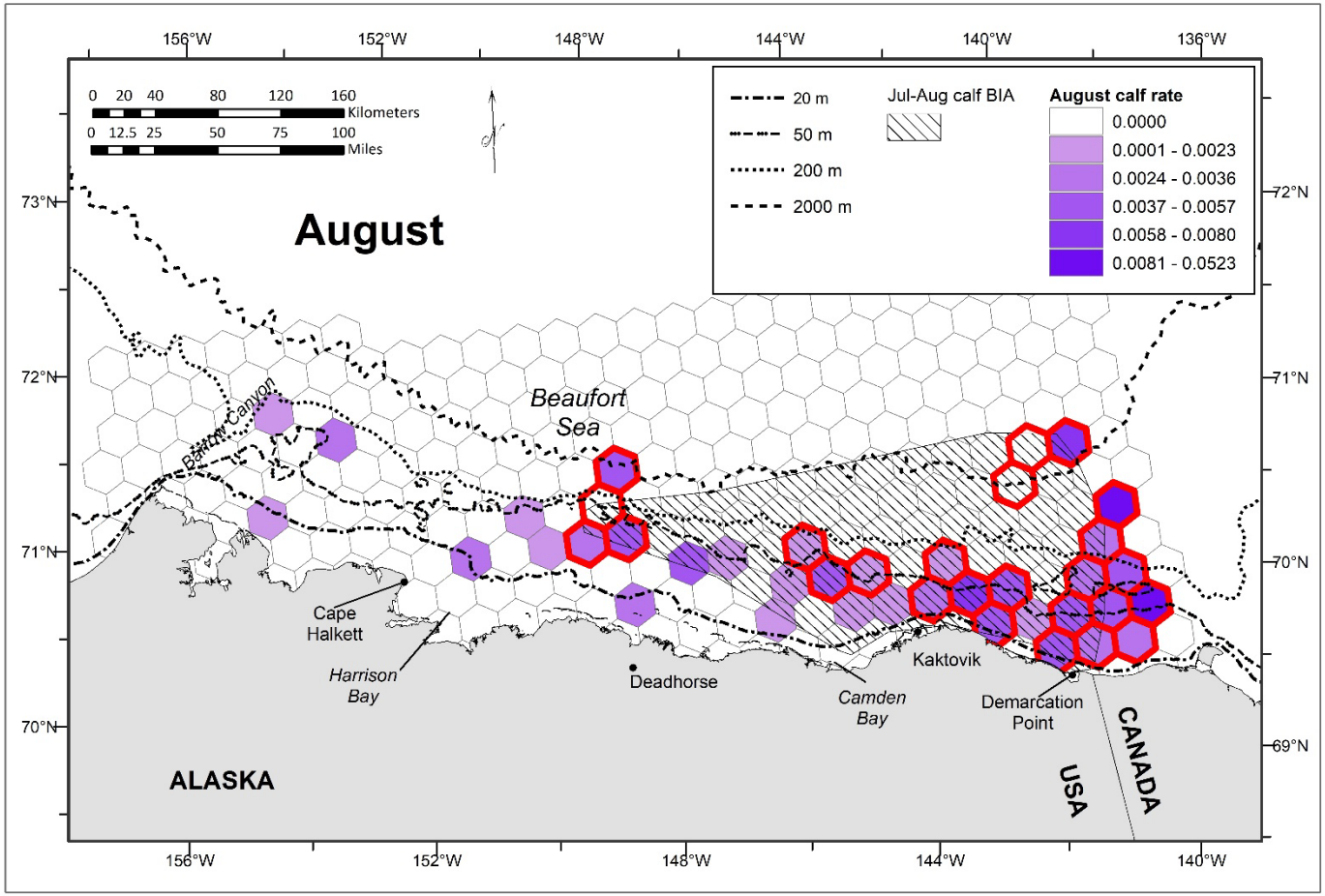

Figure S9B. Bowhead whale calf sighting rate (# calves/km) during transect and Cetacean Aggregation Protocols passing modes in the western Beaufort Sea during August from 2012 to 2019. Polygons with crosshatched shading represent the old Biologically Important Areas (BIAs) for bowhead whale calves that were delineated during the first BIA effort (Clarke et al. 2015). Red outlines surround cells chosen as the selected BIA scenarios based on the proposed optimization model results.

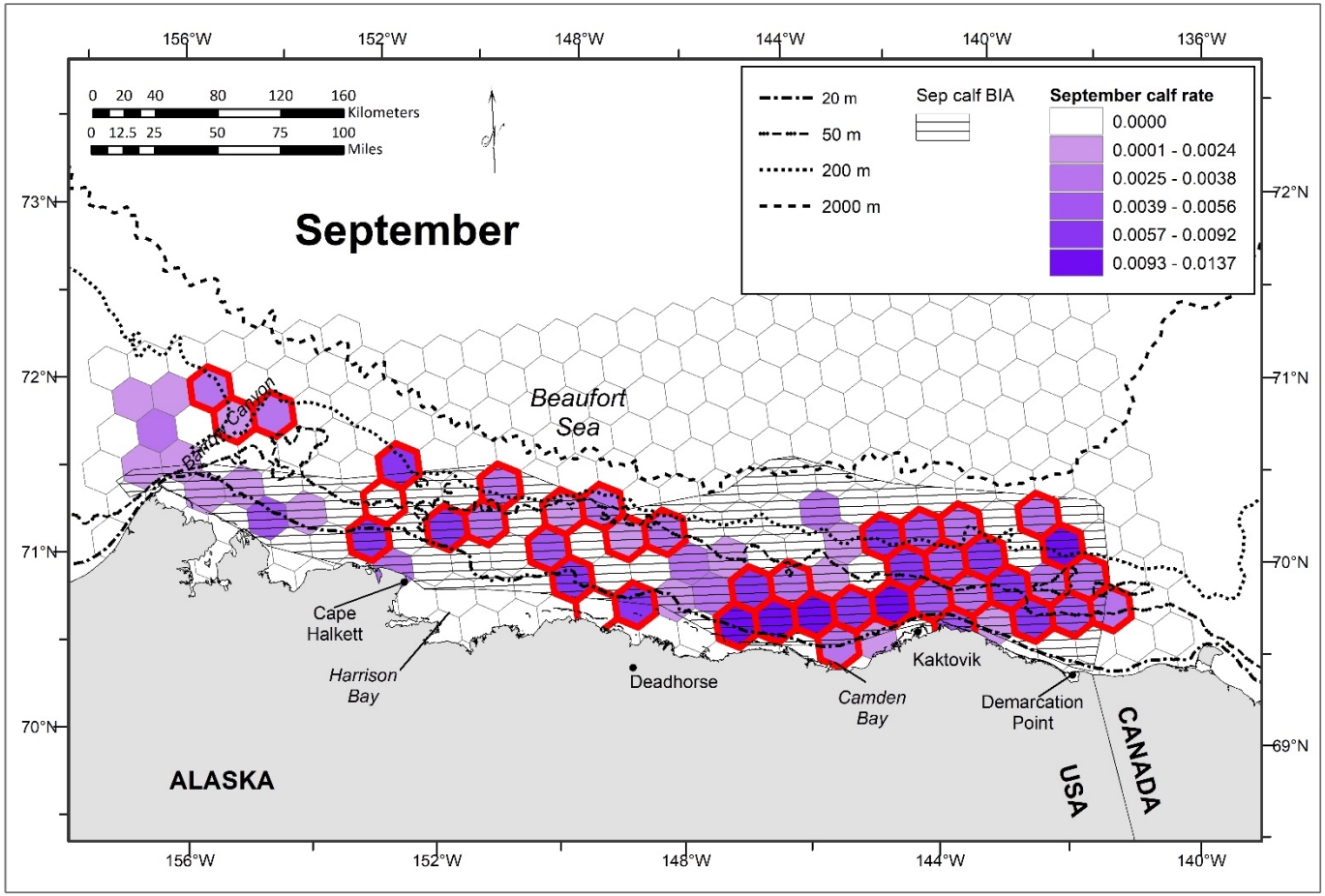

Figure S9C. Bowhead whale calf sighting rate (# calves/km) during transect and Cetacean Aggregation Protocols passing modes in the western Beaufort Sea during September from 2012 to 2019. Polygons with crosshatched shading represent the old Biologically Important Areas (BIAs) for bowhead whale calves that were delineated during the first BIA effort (Clarke et al. 2015). Red outlines surround cells chosen as the selected BIA scenarios based on the proposed optimization model results.

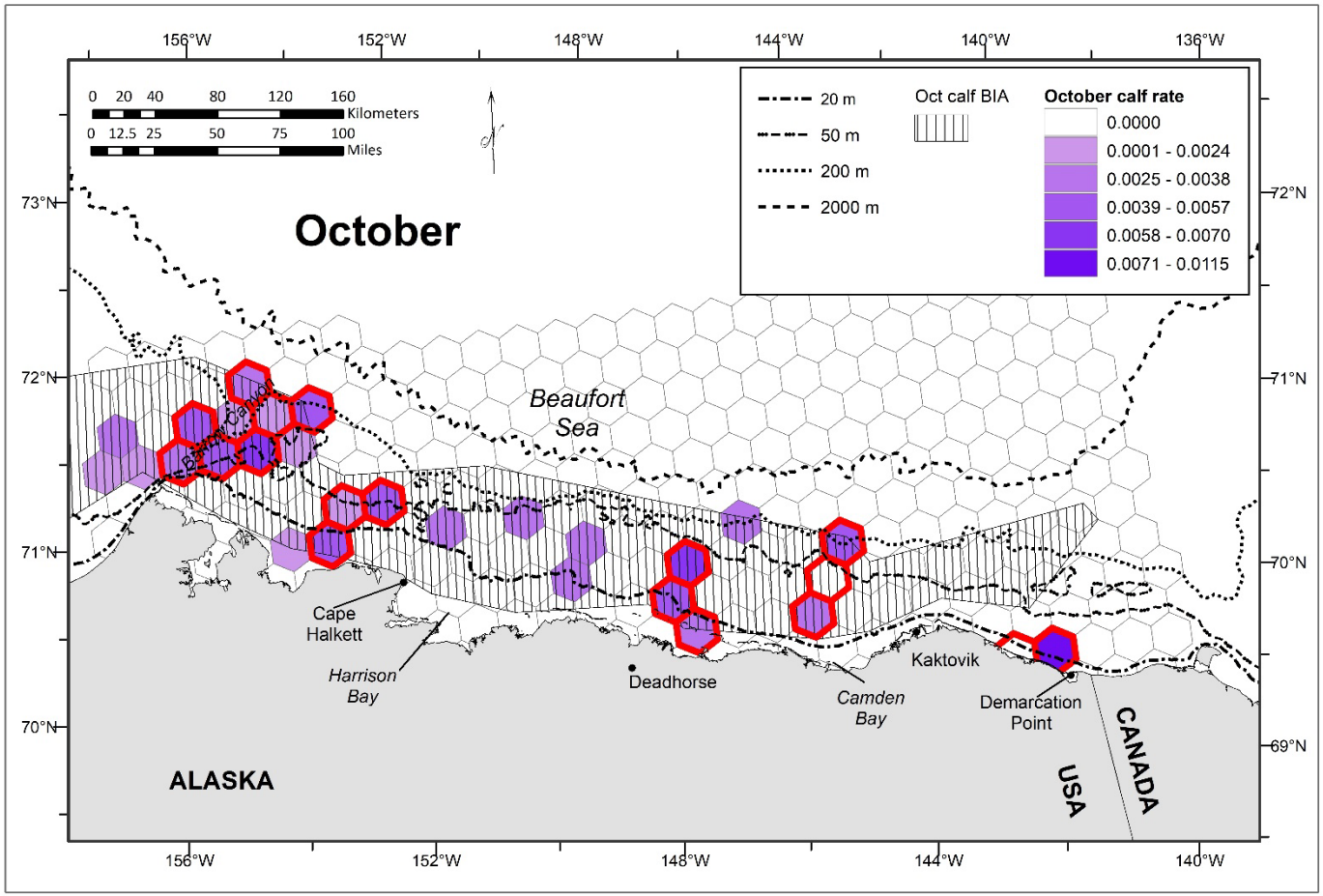

Figure S9D. Bowhead whale calf sighting rate (# calves/km) during transect and Cetacean Aggregation Protocols passing modes in the western Beaufort Sea during October from 2012 to 2019. Polygons with crosshatched shading represent the old Biologically Important Areas (BIAs) for bowhead whale calves that were delineated during the first BIA effort (Clarke et al. 2015). Red outlines surround cells chosen as the selected BIA scenarios based on the proposed optimization model results.

Literature Cited

Clarke, J. T., M. C. Ferguson, C. Curtice, and J. Harrison. 2015. Biologically Important Areas for cetaceans within the U.S. waters: Arctic region. Aquatic Mammals 41(1):94-103.